NASA TECHNICAL NOTE

NASA TN D-4920

NASA TN D-4920

RADIOFREQUENCY TRANSMISSION CHARACTERISTICS OF CANDIDATE ABLATION MATERIALS FOR PLANETARY-ENTRY-VEHICLE HEAT SHIELDS

by Melvin C. Gilreath, Andrew J. Chapman,
and Douglas M. Hatcher

Langley Research Center
Langley Station, Hampton, Va.

NATIONAL AERONAUTICS AND SPACE ADMINISTRATION • WASHINGTON, D. C. • DECEMBER 1968

RADIOFREQUENCY TRANSMISSION CHARACTERISTICS

OF CANDIDATE ABLATION MATERIALS

FOR PLANETARY-ENTRY-VEHICLE HEAT SHIELDS

By Melvin C. Gilreath, Andrew J. Chapman,
and Douglas M. Hatcher

Langley Research Center
Langley Station, Hampton, Va.

NATIONAL AERONAUTICS AND SPACE ADMINISTRATION

Page Intentionally Left Blank

RADIOFREQUENCY TRANSMISSION CHARACTERISTICS
OF CANDIDATE ABLATION MATERIALS
FOR PLANETARY-ENTRY-VEHICLE HEAT SHIELDS

By Melvin C. Gilreath, Andrew J. Chapman,
and Douglas M. Hatcher
Langley Research Center

SUMMARY

An experimental investigation was conducted to determine the radiofrequency properties of several candidate ablation materials for planetary-entry-vehicle heat shields. The radiofrequency transmissibility of each ablative material was determined by the real-time measurement of the attenuation of a 35 GHz signal while each sample was exposed to a simulated planetary entry environment. The simulated planetary environment was produced by providing a heating rate, pressure, and free-stream Mach number in an arc-heated supersonic wind tunnel. Recordings of the transmission loss obtained through each material during the arc-tunnel test and photographs of all test specimens before and after thermal exposure are presented. In addition to the transmission loss measurements, the dielectric properties of most virgin materials were measured at room temperature and are also presented.

INTRODUCTION

Highly instrumented, unmanned spacecraft will play a primary roll in the scientific exploration of neighboring planets. During atmospheric entry the spacecraft radar and radio equipment will provide such information as surface mapping, altitude, telemetry, and control commands. Antennas for such electronic equipment, as well as the primary structure of the spacecraft, must be protected from aerodynamic heating by a suitable heat-shield material. Consequently, during some phase of entry, telemetry and command control equipment may be required to transmit and receive signals through a thermally degraded heat-shield material. However, previous investigations (refs. 1 and 2) have shown that radiofrequency transmission characteristics of ablative heat-shield materials vary widely and that certain highly effective ablators severely attenuate transmission, especially after thermal degradation. Efforts are currently being made to find ablative materials which are efficient heat shields in planetary entry heating environments and are also acceptably transparent to radiofrequency transmission.

In the present investigation eleven ablative materials, which are candidates for a Martian vehicle heat shield, were tested and evaluated. Radiofrequency transmission was measured through these materials before, during, and after exposure to simulated entry-heating conditions in an arc-heated supersonic wind tunnel. Rectangular panels of the ablative test material, a transmitting antenna being attached to the back surface, were mounted in one side of a wedge-shape model. Although standard transmitting frequencies are in the range of 2 to 13 GHz, a test frequency of 35 GHz was necessary because of the antenna and model size limitations imposed by tunnel operating conditions.

Test conditions were based on two possible modes of entry into several model atmospheres which have been postulated for Mars. Entry from orbit about Mars into any of these atmospheres presents a moderate heating environment for a proposed conical vehicle of large diameter and bluntness. (See ref. 3.) This environment was simulated by a heating rate of 240 kW/m^2 and a local pressure of 0.015 atmosphere on the test panel. Direct entry into the model Martian atmospheres presents a more severe heating condition. Although such conditions can be defined only after vehicle size and shape have been determined, the test heat-transfer rate of 840 kW/m^2 should represent at least a lower bound for direct entry heating. A local pressure of 0.11 atmosphere occurred with this heat-transfer rate. The tests were conducted at a free-stream Mach number of 3.4 to 3.5, and total enthalpy between 6.3 and 6.5 MJ/kg.

Other ablator properties affecting antenna performance were measured in addition to the transmission loss characteristics measured during simulated entry heating. The dielectric constant and loss tangent of each ablator were measured before testing in the arc tunnel, and transmission losses through the ablative test panels were measured in an anechoic chamber before and after testing in the arc tunnel.

SYMBOLS

L_C transmission loss through thermally degraded test specimen after cooling, dB

L_H transmission loss through thermally degraded test specimen before cooling, dB

M_∞ free-stream Mach number

$p_{t,1}$ total pressure, kN/m^2

$p_{t,2}$ model stagnation pressure, kN/m^2

p_2 model pressure, kN/m^2

2

q_o model stagnation-point heat-transfer rate, MW/m^2

q heat-transfer rate, MW/m^2

r model nose radius

s surface distance from stagnation point

$\tan \delta$ loss tangent of dielectric medium

w mass flow, kg/sec

α angle of attack, radians

θ flow deflection angle, radians

ϵ_r relative dielectric constant

ρ density of material, kg/m^3

DESCRIPTION OF TEST MODELS

Details of the model used to test ablators for radiofrequency transparency are shown in figure 1. This model is a 0.32-radian half-angle wedge with a 7.262-centimeter span and 9.85-centimeter chord length. This type of model was chosen primarily because it allowed the use of a rectangular test panel. The rectangular test panel was the least expensive to construct and it was also more desirable for the radiofrequency transmission measurements. The model consists of a stainless-steel core covered by an inconel skin. The model is cooled by water circulating through passages machined in the core. The ablative test panel is mounted in a cavity which is open on one side of the test model. The front surface of the ablative panel fits into this opening and is retained flush with the model surface by a flange formed by the inconel skin. The test panel is supported from the back by a ramp which slides longitudinally into the model. The position of the ramp is adjustable so that test panels of varying thickness can be mounted in the model.

The ablative test panel is bonded to an inconel substrate. A 35 GHz horn antenna having an aperture size of 1.003 cm by 1.956 cm was attached over an opening in the substrate and was connected to a klystron signal source by a flexible waveguide with internal dimensions of 0.356 cm by 0.711 cm.

3

Calibration models, identical in size and shape to the test models, were used to measure pressure and heat transfer over the surface of the wedge shape. Details of the pressure model are shown in figure 2. Nine pressure orifices were installed on the surface of the model along the center line. Locations of the orifices are identified by the ratio of surface distance from the stagnation point to model nose radius s/r. The orifices were connected to pressure transducers by flexible metal tubing. The model was constructed of stainless steel and inconel and cooled by circulating water.

Details of the heat-transfer model are shown in figure 3. This model was a thin wall-type calorimeter. Thermocouples were attached to the back surface of the 0.762-millimeter-thick inconel skin at the positions shown in figure 3. Heat-transfer rates at these points were determined from temperature-rise rate and properties of the inconel skin.

Figure 4 shows the three models mounted in the tunnel in preparation for testing. Each model is mounted on a strut which moves radially to position the model into or out of the stream. The upper photograph of figure 4 shows the radiofrequency transparency model in position for testing. The horn antenna, which receives the signal transmitted through the ablator during tunnel operation, is alined with the transmitting antenna behind the ablative panel. The lower photograph of figure 4 shows the radiofrequency transparency test model in the test position and the two calibration models in the stowed position.

TEST CONDITIONS AND PROCEDURES

Measurements of Dielectric Properties of Virgin Materials at Room Temperature

The dielectric properties of most virgin test materials were measured at room temperature at two frequencies within the frequency range of approximately 2 to 13 GHz. This frequency range was chosen since most spacecraft antenna systems being considered for future missions operate within this range with increasing emphasis on the 8.2 to 12.4 GHz range. Two techniques were used to accomplish the measurements since neither of the two available instrumentation setups, with existing components, could cover the entire frequency range. A coaxial nonslotted line technique (ref. 4) was used from 2 to 6 GHz and the lowest order mode rectilinear cavity method (refs. 5 and 6) was used from approximately 9 to 13 GHz.

The radiofrequency-transmission-loss measurement test frequency of 35 GHz is higher than that used for measuring the dielectric properties and further discussion concerning the selection of this frequency is presented in a subsequent section. Dielectric properties at room temperature of several materials have been measured (ref. 7) at 35 GHz. The values of dielectric constant and loss tangent obtained at 35 GHz, for those

4

materials measured, do differ somewhat from those measured at the lower frequencies; however, these differences appear to be small.

For this test program, values of dielectric constant and loss tangent measured over the 9 to 13 GHz frequency range are assumed to be approximately correct at 35 GHz.

Tunnel Tests

Tunnel operation.- Radiofrequency transmission through the ablators was measured at two different tunnel operating conditions which are described in table I. Stagnation enthalpy and Mach number did not differ greatly at these test conditions. For the low heat-transfer condition, the model was at zero angle of attack in the test stream. However, the heat-transfer rate on the test panel (s/r > 4) was approximately quadrupled by increasing the angle of attack to 0.49 radian and increasing total pressure somewhat. Heat-transfer distribution is shown in figure 5 and pressure distribution is shown in figure 6.

Photographs of models in the test stream are shown in figures 7 and 8. The deflection angle of 0.32 radian at zero angle of attack (figs. 7(a) and 8(a)) produced a relatively weak shock and low pressure recovery over the wedge afterbody. The deflection angle of 0.812 radian at an angle of attack of 0.49 radian (fig. 7(b)) produced a very strong shock and high pressure recovery and accounted for the higher heat-transfer rate. In figure 7(b), the model leading edge is shown very close to the stream edge; this position was necessary to obtain a profile view. For ablator transmission tests, the model was rotated and moved closer to the center of the stream as shown in figure 8(b).

Radiofrequency transmission test.- The size of the test model (fig. 1) chosen for the radiofrequency transmission test was limited by the arc-tunnel test facility and the desired test conditions. Because of this test-model-size limitation, restrictions were placed on the test antenna size and therefore, the test frequency. An antenna having half-power beam widths of 45° or less was required in order that reflections inside the arc tunnel be reduced as much as possible during the thermal test. The small beam widths were also desirable because the smaller the beam width the less influence the test specimen size has on the antenna performance.

To satisfy the antenna beam-width requirement, within the restrictions imposed by the test model size, frequencies in the 26.5 to 40 GHz range were considered for the radiofrequency transmission test. The design of a small horn antenna could be achieved that would satisfy all these requirements. Signal sources were also available that would provide the necessary output power for the thermal test. The test frequency was chosen as 35 GHz because, as stated earlier, the antenna requirements could be satisfied and existing instrumentation was available.

A simplified block diagram of the instrumentation setup for making the transmission loss measurements in the arc tunnel is shown in figure 9. A 35 GHz klystron modulated with a 1.0 kHz square wave was used as the transmitting source providing output power in excess of 1 watt. This signal was transmitted through a rectangular waveguide into the test section of the arc tunnel to the water-cooled test model. The forward power was monitored by utilizing a directional coupler, crystal detector, and power meter. The signal was transmitted from the test model through the test specimen and received by a horn antenna positioned (fig. 4) to receive maximum signal level. A crystal envelope detector was used at the output of the receiving antenna to detect the received signal which, in turn, was then recorded on a 1-kHz ac recorder having a 40-dB dynamic range. The recorder also had a chart time base that was adjusted to provide the desired recording speed for each test.

The radiofrequency-transmission measurements in the arc tunnel were made by using the following procedure. With the model located in the test position, as shown in figures 4 and 9, and with the transmitting source operating, the recorder was adjusted to the desired calibration level before arc ignition. This calibration level does not include any transmission loss through the virgin material and is used only as a reference for determining the transmission loss during and after thermal degradation of the test specimen. After the desired calibration level was obtained, the arc-heater magnetic field was turned on without arc ignition to determine what effect this field would have on the received signal level. The only observed magnetic-field effects were small changes in the received-signal amplitude. After the calibration level and field effects were recorded, the test model was removed from the test position. The arc was ignited and the proper adjustments were made to provide the conditions indicated in table I. The calorimeter and pressure models were then inserted to measure the stream conditions. Upon completion of the stream measurements, the model was inserted and the thermal test began. The time for all low heat-transfer tests was 60 seconds except for one test of 49 seconds. The time for the high heat-transfer tests was 30 seconds for all specimens.

At the end of each thermal test, the specimen was allowed to remain in the test position and cool for 240 seconds while the transmission loss was being recorded. The cooling period of 240 seconds was chosen because the air flow around the model could be maintained and the pressure inside the test section would remain essentially constant for this period.

Anechoic Chamber Tests

The transmission loss through each virgin material was measured prior to the thermal test at the test frequency of 35 GHz in an anechoic test chamber. Each specimen was mounted in a test model similar to that used for the thermal test and the antenna gain was determined by comparing it with a known reference antenna. This value was then

compared with that obtained with no specimen. The difference between the antenna gain obtained with no specimen and that measured when the antennas were covered with a specimen is defined as the loss through the virgin material. The specimen was enclosed on all edges with a conducting shield to eliminate any errors due to radiation from the specimen edges.

These measurements were repeated on the thermally degraded specimens after they were removed from the arc tunnel and the transmission loss for each specimen was obtained.

RESULTS AND DISCUSSION

Dielectric Properties of Virgin Materials

The results of the room-temperature dielectric constant and loss tangent measurements for most test specimens are given in table II. The frequency at which these measurements were made did not remain constant but changed from one material to another because the resonant frequency of the loaded test cavity changed with a change in dielectric constant of the test specimen.

Some of the materials (that is, foamed teflon, B47 RF, and poly carborazole) were rather flexible and difficulties were encountered in machining the test specimens that were used for determining the dielectric properties of these materials. These machining problems made it extremely difficult to obtain test specimens having the proper tolerances for measurement of the dielectric properties; therefore, there may be small errors in the values presented for these materials in table II. The Martin SLA-561 material was very inhomogeneous and the dielectric constant and loss tangent values presented in table II for this material represent an average of a number of measurements of different samples. The dielectric properties of some of the materials (that is, Avcoat 5026-39 HCG and E4A1) have been measured and the results published in previous work (refs. 2 and 8); however, the properties of the materials used in this test program were measured again since they do vary occasionally from one specimen to another. No attempt was made to measure the dielectric properties of the materials after thermal exposure because severe degradation of most test specimens made it impossible to machine samples having the tolerances required for these measurements.

Virgin Material Transmission Loss Measurements in Anechoic Chamber

The results of the virgin-material transmission-loss measurements conducted in the anechoic chamber are presented in table III and are given only to indicate the approximate transmission loss through each material. These losses have not been corrected for variations in the transmitting antenna impedance that occurred when the different

specimens were placed over the antenna. Measurements of these impedance variations indicated that changes in the losses that could be attributed to this mismatch when changing from the no-specimen to the specimen condition were in the order of ±0.5 dB or less for most materials. Therefore, the actual transmission loss could be slightly larger or smaller than the values presented in table III. The Martin SLA-561 material was the only virgin material having high losses.

Radiofrequency-Transmission Tests in Arc Tunnel

The results of the arc-tunnel transmission-loss measurements are presented in tables IV and V. The transmission losses for all materials exposed to the low-heat-transfer test condition are given in table IV and those for the high-heat-transfer test condition are given in table V. Higher density materials, such as Avcoat 5026-39 HCG and Mod 7, are, in general, of interest only for the more severe heating conditions and therefore were not exposed to the low heating-rate test. The Avco foamed teflon and McDonnell B47 RF materials were not exposed to the high heating rate because the considerable loss of material during the low-heating-rate test indicated they would not survive the more severe heating conditions. No data were obtained for the E6A7 material during the high-heating-rate test because of mechanical problems encountered during the test.

Two loss values are presented in tables IV and V for each test specimen. The loss number designated as "hot" is that value obtained immediately after the jet is turned off and the "cold" value is that obtained at the end of a 240-second cooling period. Given in the extreme right-hand columns of tables IV and V are figure numbers relating each specimen to a transmission loss recording obtained during the thermal test. These transmission loss records are presented in figures 10 and 11 for the low- and high-heat-transfer conditions, respectively. Figures 10 and 11 should be reviewed in conjunction with tables IV and V in order to understand clearly the significance of the loss values presented. The test data obtained during the thermal test of most materials appear to be free of any interference effects created by the high energy stream. However, for some of the materials that produced high transmission losses, there is some noise present on the test records during that portion of the thermal test after the loss exceeded approximately 10 to 12 dB.

The transmission loss recordings for McDonnell B47 RF (fig. 10(e)) show a sudden change in transmission loss during the arc-tunnel test for both specimens. This sudden change was caused when the leading edge of the char layer peeled away, was deposited over the transmitting antenna, and created a sudden increase in transmission loss.

Peculiarities occurring during tests of some of the other materials are explained on the records (figs. 10(i), 11(d), and 11(h)).

Thermally Degraded Material Transmission Loss

Measurements in Anechoic Chamber

The results of the transmission loss measurements through the materials after thermal exposure, for both low- and high-heat-transfer test conditions, are given in table VI. There is generally good agreement between these values and the cold transmission loss values presented in tables IV and V. Most of the discrepancies occurred for materials having high losses in their virgin state, such as Martin SLA-561 and Avco Mod 7. The cold transmission loss values measured in the arc tunnel for these materials are, in general, less than those values obtained in the anechoic chamber measurements and these differences are attributed to the transmission loss produced by the remaining virgin material. It was necessary to use different references for the two measurements. For the arc-tunnel tests the reference (0-dB transmission loss) level was obtained while transmitting through the test specimen in its virgin state prior to thermal exposure and thereby ignoring any virgin material loss during the thermal test; thus, only the change in transmission loss due to thermal degradation of the test specimen is obtained. For the anechoic chamber tests, the reference (0-dB transmission loss) used was the transmitting antenna with no test specimen; in which case when the thermally degraded specimen is measured, the total transmission loss through both the remaining virgin material and charred material is obtained. If an estimate of the transmission loss through the remaining virgin material for these thermally degraded materials could be obtained and added to the arc-tunnel cold transmission loss values, they should agree very closely with those values obtained in the anechoic chamber measurements.

Test Specimen Photographs

Photographs of all test specimens before and after arc-tunnel testing are presented in figures 12 and 13. Photographs of the low-heat-transfer test specimens are given in figure 12 and those for the high-heat-transfer test condition in figure 13. The top photograph of each figure shows the test material in its virgin condition and the remaining photographs are those of the different specimens after exposure to the arc-tunnel test. For example, figure 12(a) consists of three photographs. The top photograph is that of the virgin material, the middle photograph shows test specimen 1 after thermal exposure, and the bottom photograph shows test specimen 2 after thermal exposure. Some figures, such as figures 13(e) and 13(h), only have two photographs since only one specimen was measured for that particular test.

CONCLUDING REMARKS

Real-time radiofrequency-transmission-loss measurements through several candidate ablation materials for entry-vehicle heat shields were made in an arc-heated supersonic wind tunnel. In addition, radiofrequency transmission losses through all test materials were measured in an anechoic test chamber before and after testing in the arc tunnel. The transmission-loss measurements indicate that ablation materials which form and retain appreciable conducting char layers during thermal degradation, in general, produce very high radiofrequency transmission losses. Several elastomeric materials retained a uniform char layer at low-heat-transfer conditions while producing low transmission loss. Other materials, including foamed teflon exhibited low transmission losses; however, high material loss during low heating rate tests indicated low thermal shielding performance for these materials.

Although all the radiofrequency performance data presented for the ablation materials considered in this test program were measured at 35 GHz, the performance of the materials is expected to improve when used in the frequency range of 2GHz to 13 GHz. In order to determine the actual performance of these materials in the frequency range of 2 GHz to 13 GHz, additional analytical and experimental work would be required.

Langley Research Center,
    National Aeronautics and Space Administration,
        Langley Station, Hampton, Va., Sept. 5, 1968,
            125-22-02-02-23.

REFERENCES

1. Dow, Marvin B.; Pittman, Claud M.; and Croswell, William F.: Thermal Performance and Radio-Frequency Transmissivity of Several Ablation Materials. NASA TN D-1896, 1964.

2. Gilreath, Melvin C.; Croswell, William F.; and Castellow, Stark L., Jr.: Radiofrequency Transmission Characteristics of Several Ablation Materials. NASA TN D-4879, 1968.

3. Vosteen, Louis F.: Heat-Shield Materials Development for Voyager. Paper presented at Third International Symposium on High Temperature Technology, Sept. 1967.

4. Spalding, H., ed.: Die Kurz Information 3/4. Rohde & Schwarz (Passaic, N.J.), 1962.

5. Altschuler, H. M.: Dielectric Constant. Handbook of Microwave Measurements, Third ed., Vol. II, Max Sucher and Jerome Fox, eds., Polytech. Press of Polytech. Inst. Brooklyn, c.1963, pp. 495-548.

6. Ginzton, Edward L.: Microwave Measurements. McGraw-Hill Book Co., Inc., 1957.

7. Hakki, B. W.; and Coleman, P. D.: A Dielectric Resonator Method of Measuring Inductive Capacities in the Millimeter Range. IRE Trans. Microwave Theory and Tech., vol. MTT-8, no. 4, July 1960, pp. 402-410.

8. Trousdale, J. E.: A Study of Ablation Material Effects on Antenna Performance. RAD-TR-66-4 (Contract NAS 9-4916), AVCO Corp., Feb. 11, 1966.

TABLE I.- CONDITIONS FOR ABLATOR RADIOFREQUENCY TRANSPARENCY TESTS

FOR 0.65-RADIAN WEDGE MODEL

[Test medium, air]

	Low heat transfer	High heat transfer
Mass flow, w, kg/sec	0.14	0.16
Arc power, kw	2200	2550
Free-stream Mach number, M_∞	3.4	3.5
Total enthalpy, MJ/kg	6.51	6.28
Total pressure, $p_{t,1}$, kN/m^2	203	238
Angle of attack, α, radians	0	0.49
Flow deflection angle, θ, radians	0.32	0.81
Model pressure, p_2, kN/m^2, for model positions:		
s/r = 0	15.20	12.36
s/r = 4	2.43	12.97
s/r = 8	1.52	10.64
s/r = 12	1.01	9.12
Heat-transfer rate, q, MW/m^2, for model positions:		
s/r = 0	2.02	1.71
s/r = 4	0.31	0.91
s/r = 6	0.24	0.84
s/r = 8	0.22	0.89
s/r = 10	0.19	0.86
s/r = 12	0.17	0.78

TABLE II.- PROPERTIES OF VIRGIN MATERIALS AT ROOM TEMPERATURE

Material	Frequency, GHz	Dielectric constant, ϵ_r	Loss tangent, tan δ	Density, ρ, kg/m^3
Avco foamed teflon[a]	5.36	1.29	0.0037	576.753
	12.74	1.23	.001	
Avco 893-23[b]	2.35	1.62	.0219	445.305
	10.98	1.66	.0154	
Avcoat 5026-99A[c]	2.38	1.64	.0275	363.701
	11.36	1.55	.0135	
Avcoat 5026-39 HCG[c]	5.23	1.86		495.523
	10.59	1.79	.030	
Boeing poly carborazole[e]	5.06	1.79	.0247	508.365
	10.48	1.82	.0171	
McDonnell B47 RF[d]	4.84	1.62	.0124	391.550
	11.16	1.61	.0177	
Martin SLA-561[b,f]	4.23	1.96		178.860
	9.32	2.31	.0896	
E4A1[d]	5.89	2.06		682.995
	9.93	2.03	.0311	
E6A7[d]	4.20	2.30		564.850
	9.52	2.21	.0284	

[a]Subliming ablator.

[b]Cork composite.

[c]Rigid charring ablator.

[d]Silicone elastomer.

[e]Special composite.

[f]Inhomogeneity of this material produced a variation in both the dielectric constant and loss tangent from one test sample to another and the values presented are an average of a number of measurements.

TABLE III.- TRANSMISSION LOSSES THROUGH VIRGIN MATERIALS

MEASURED AT 35 GHz IN ANECHOIC CHAMBER

Material	Transmission loss, dB (*)	Material thickness, cm
Avco foamed teflon	0.1	0.879
Avco 893-23	0	.767
Avcoat 5026-99A	1.0	.769
Avcoat 5026-39 HCG	0	.742
Avco Mod 7	2.8	.800
Boeing poly carborazole	.6	.721
McDonnell B47 RF	.6	.767
Martin SLA-220	.2	.769
Martin SLA-561	7.8	.767
E4A1	1.4	.762
E6A7	2.2	.765

*Measurement accuracy ±0.5 dB.

TABLE IV.- RESULTS OF TRANSMISSION-LOSS MEASUREMENTS IN ARC TUNNEL

FOR LOW-HEAT-TRANSFER TEST CONDITION

$[\alpha = 0 \text{ rad}]$

Test material	Specimen	Material thickness over test antenna		Transmission loss, dB		Figure
		Before test, cm	After test, cm	Hot	Cold	
Avco foamed teflon	1	0.879	0.264	1	<1	10(a)
	2	.843	.241	<1	<1	
Avco 893-23	1	.769	.886	16	11	10(b)
	2	.775	.866	23.6	15.6	
Avcoat 5026-99A	1	.769	.668	27	23	10(c)
	2	.777	.688	29.2	23.8	
Boeing poly carborazole	1	.721	.508	9.4	6.4	10(d)
	2	.716	.546	19.4	13.6	
McDonnell B47 RF[*]	1	.767	.267	4.6	3.0	10(e)
	2	.731	.318	7.2	3.5	
Martin SLA-220	1	.769	.737	2.0	<1	10(f)
	2	.767	.693	1.9	<1	
Martin SLA-561	1	.767	.739	20	19	10(g)
	2	.775	.742	22.4	21.2	
E4A1	1	.762	.866	1.8	2.4	10(h)
	3X	.762	.869	2.4	2.0	
E6A7	1	.765	.538	5.0	0 (±0.5)	10(i)

[*]Test time for this material was 49 seconds.

15

TABLE V.- RESULTS OF TRANSMISSION-LOSS MEASUREMENTS IN ARC TUNNEL

FOR HIGH-HEAT-TRANSFER TEST CONDITION

$$[\alpha = 0.49 \text{ rad}]$$

Test material	Specimen	Material thickness over test antenna		Transmission loss, dB		Figure
		Before test, cm	After test, cm	Hot	Cold	
Avco 893-23	3	0.782	0.892	24	19.2	11(a)
	4	.792	.879	20.6	19.3	
Avcoat 5026-99A	3	.772	.704	36+	36+	11(b)
	4	.772	.704	36+	36+	
Avcoat 5026-39 HCG	1	.742	.706	36+	36+	11(c)
	2	.757	.724	35+	33.8	
Avco Mod 7	1	.800	.884	33	20.6	11(d)
	2	.762	.577	36	24.6, 0.4*	
Boeing poly carborazole	3	.701	.437	18	13.3	11(e)
Martin SLA-220	3	.765	.315	3.6	2.1	11(f)
	4	.765	.315	4.6	.6	
Martin SLA-561	3	.767	.714	32.6	27.5	11(g)
	4	.775	.719	32.8	30.5	
E4A1	1X	.775	.582	15.8	1.6	11(h)

*Low transmission loss for this specimen was due to loss of char layer during cooling period in arc tunnel.

TABLE VI.- TRANSMISSION LOSSES THROUGH TEST MATERIALS MEASURED IN ANECHOIC CHAMBER AFTER THERMAL EXPOSURE

Test material	Low heat transfer ($\alpha = 0$ rad)		High heat transfer ($\alpha = 0.49$ rad)	
	Specimen	Loss, dB	Specimen	Loss, dB
Avco foamed teflon	1	0 (± 0.5)		
	2	0 (± 0.5)		
Avco 893-23	1	13.5	3	22.5
	2	14.0	4	22.0
Avcoat 5026-99A	1	26	3	35+
	2	25	4	35+
Avcoat 5026-39 HCG			1	35+
			2	35+
Avco Mod 7			1	26
			2	[a]1
Boeing poly carborazole	1	5.5	3	17
	2	12		
McDonnell B47 RF	1	2		
	2	0 (± 0.5)		
Martin SLA-220	1	.5	3	.5
	2	.5	4	.5
Martin SLA-561	1	24	3	32
	2	26	4	32
E4A1	3X	4.0	X	.8
	1	4.0		
E6A7	1	2.0		

[a]Low transmission loss for this specimen was due to loss of char layer during cooling period in arc tunnel.

Figure 1.- Details of radiofrequency transparency test model. Dimensions are in centimeters.

Pressure orifices

Inconel skin

8.19

5.14

2.09

4

1.25

0.76 Radius

s/r = 0

0.57 1.25

2

3.62

6

6.66

10

12

8

0.32 radian

Cooling water passage

Stainless—steel core

Sting attachment

Monel tubing

Section view

9.85

7.62
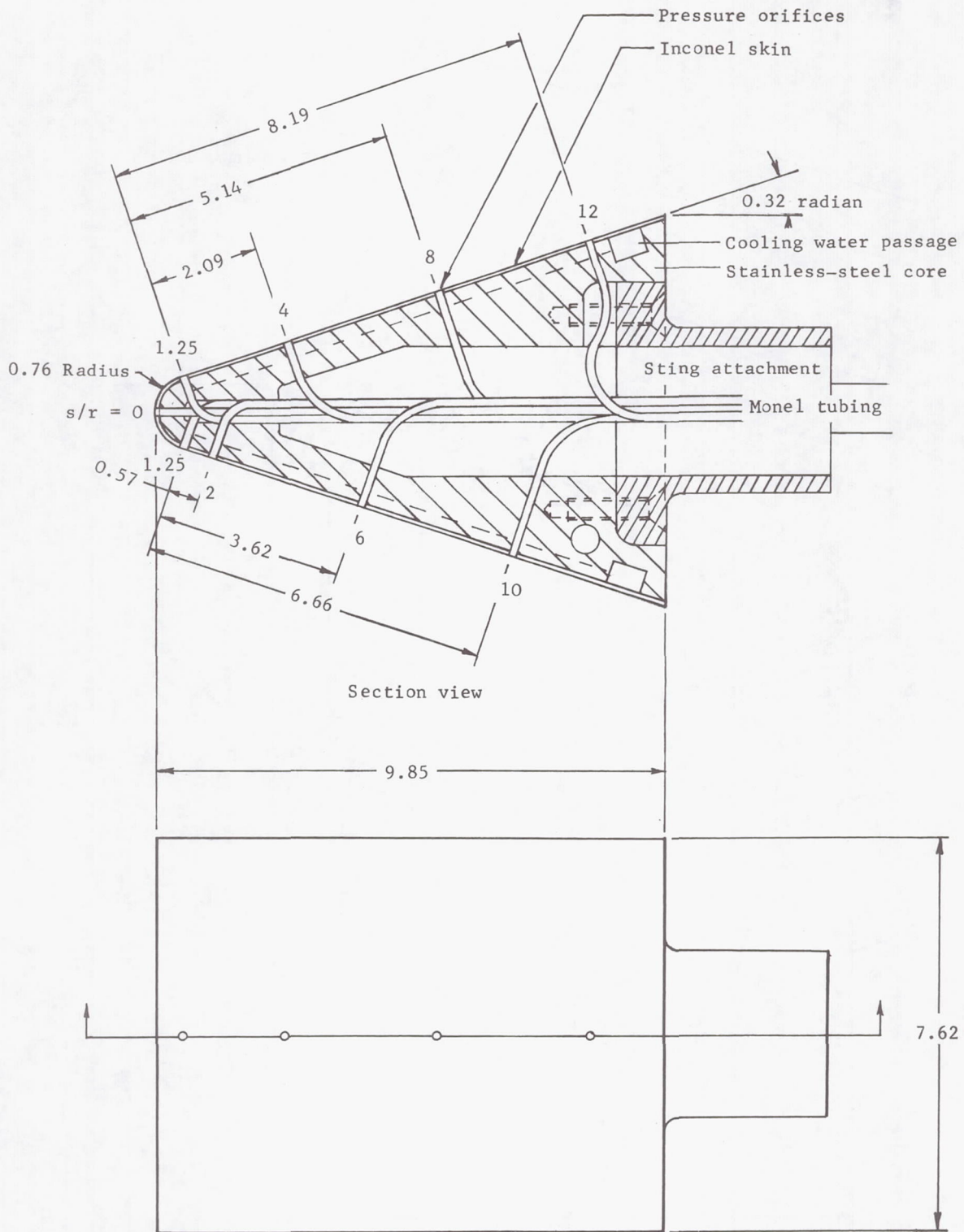
Figure 2.- Details of pressure model. Dimensions are in centimeters.
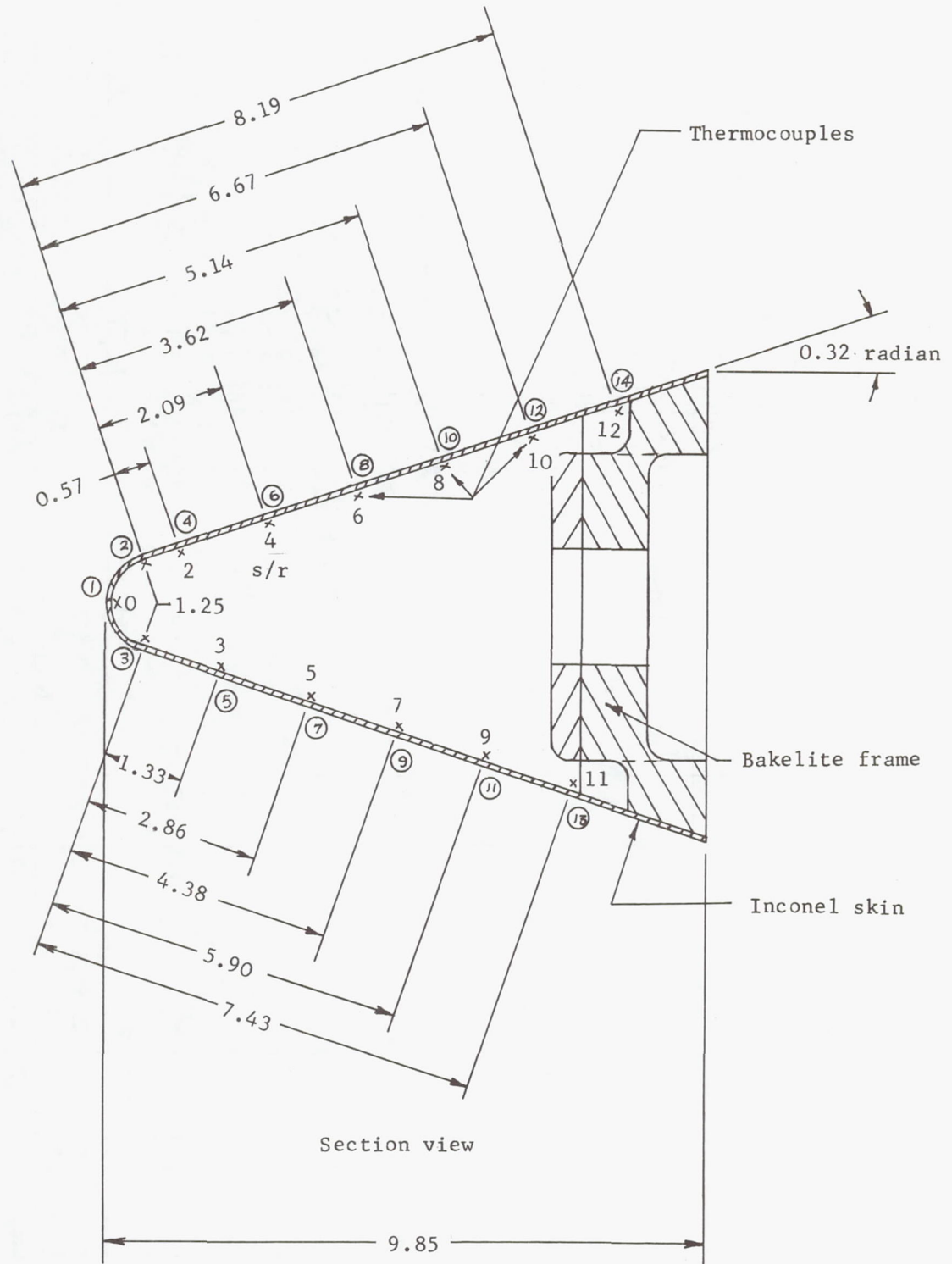
Figure 3.- Details of heat-transfer model. Dimensions are in centimeters.

Nozzle

Receiving antenna

Pressure model

Radiofrequency
transparency model

(a) View looking upstream.

Pressure model

Nozzle

Heat-transfer model

Radiofrequency
transparency model
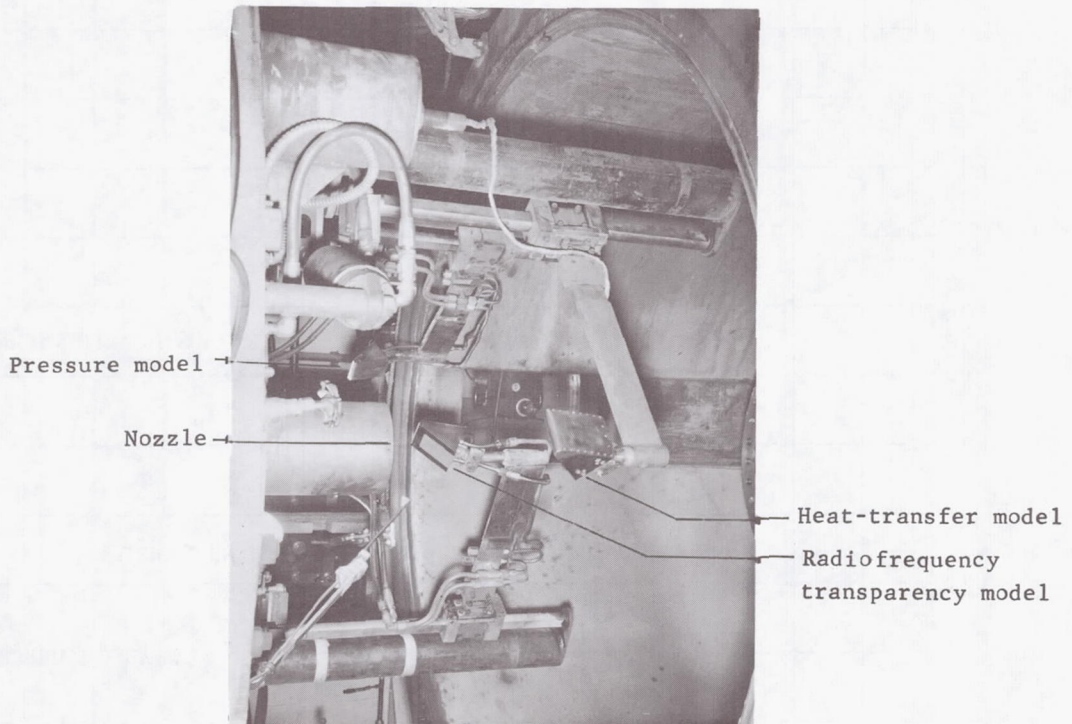
(b) View looking downstream.   L-68-8516

Figure 4.- Photographs of 0.65-radian wedge model installed in tunnel.
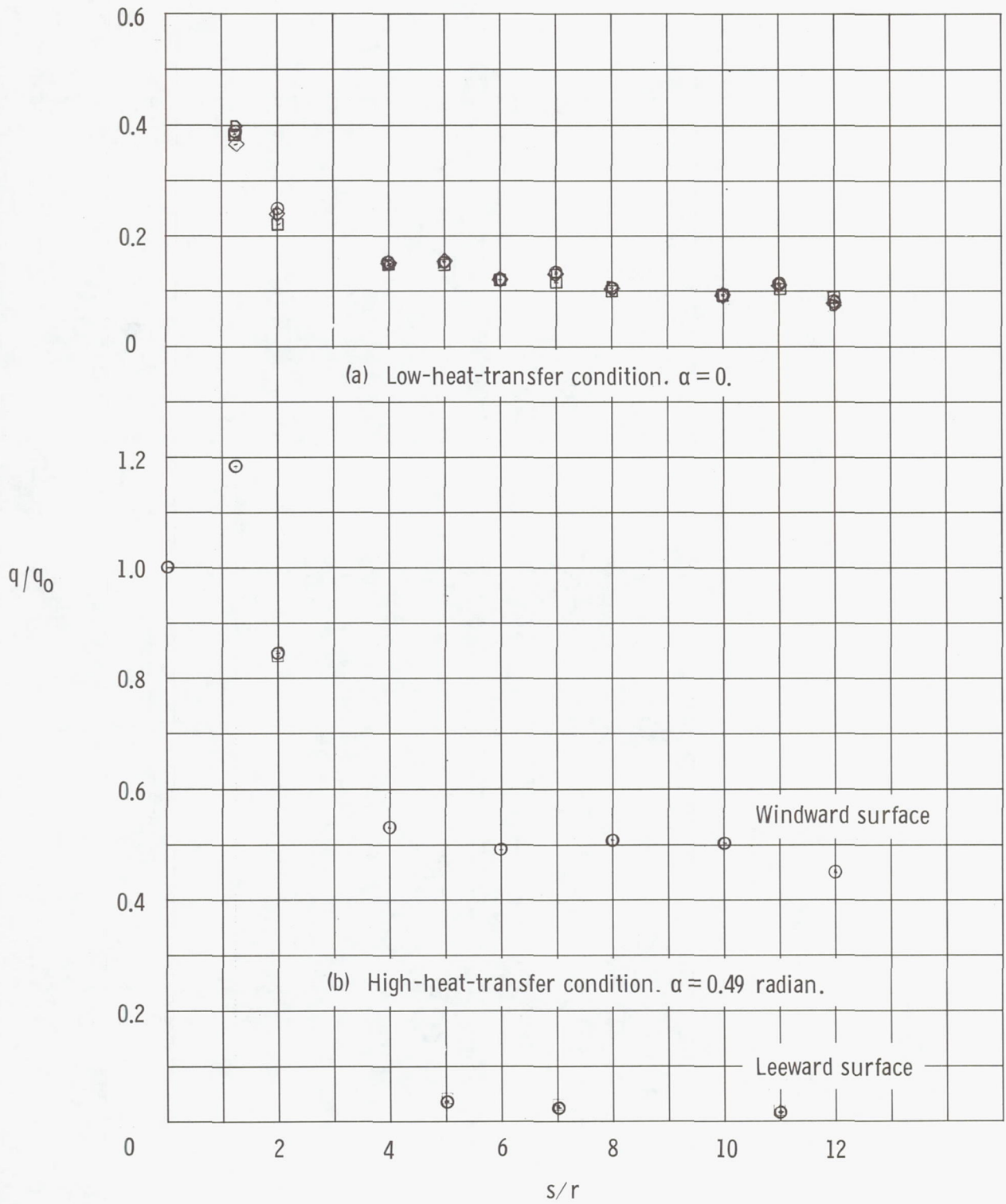
Figure 5.- Heat-transfer distribution on 0.65-radian wedge.
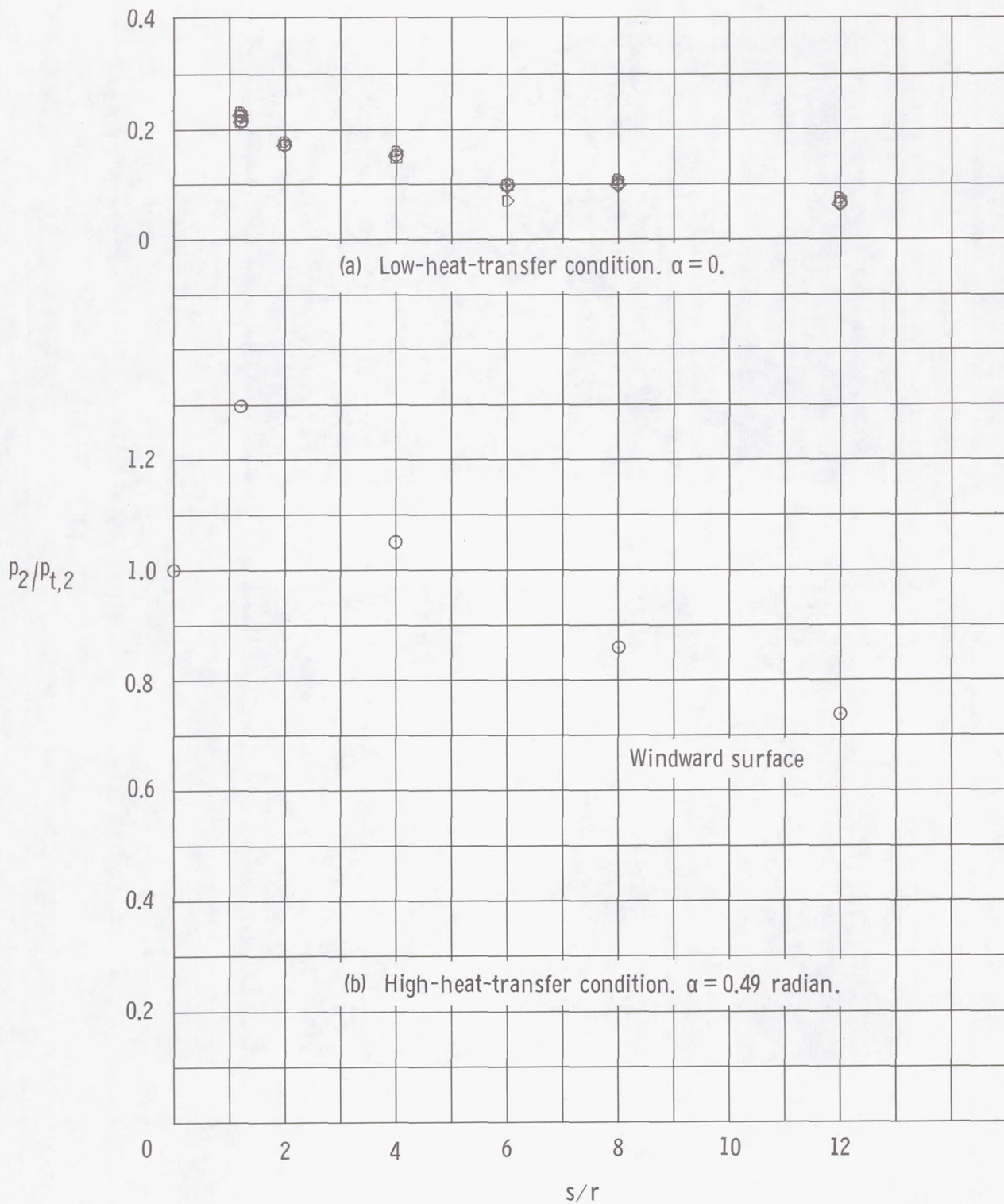
Figure 6.- Pressure distribution on 0.65-radian wedge.

.23

(a) Low-heat-transfer condition. α = 0.

(b) High-heat-transfer condition. α = 0.49 radian.

L-68-8517

Figure 7.- Photographs of 0.65-radian wedge models in test stream.
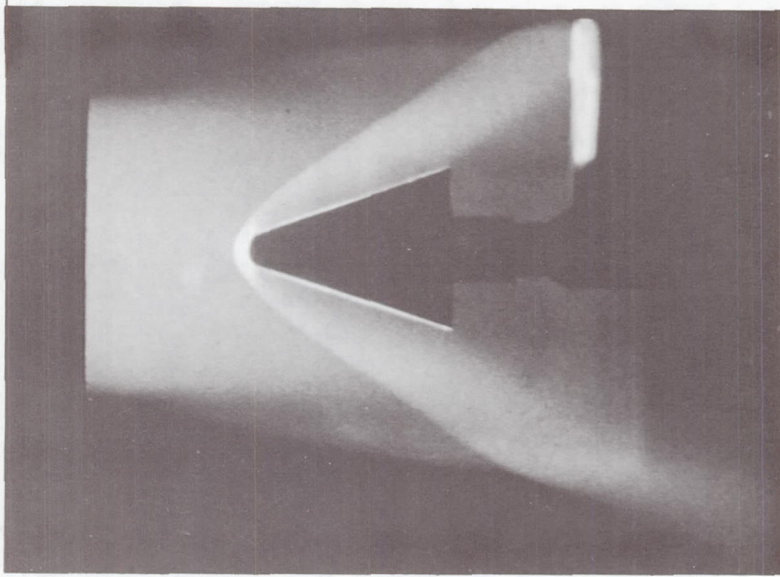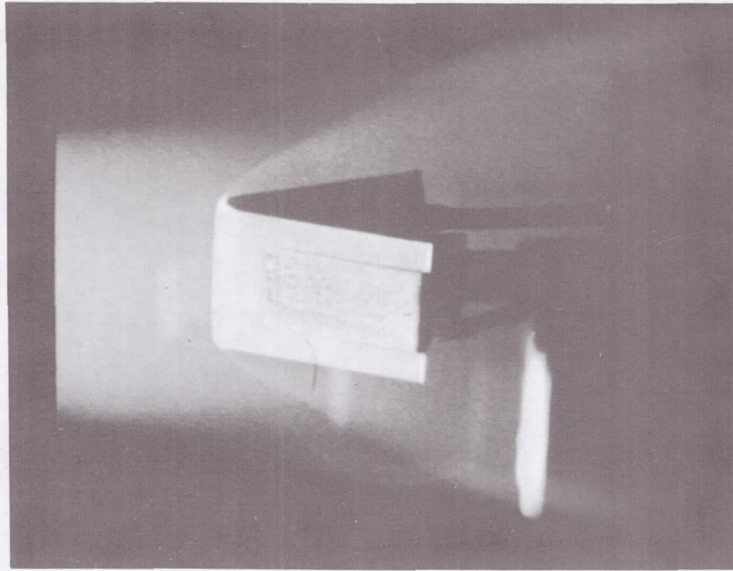
(a) Low-heat-transfer condition. $\alpha = 0$.
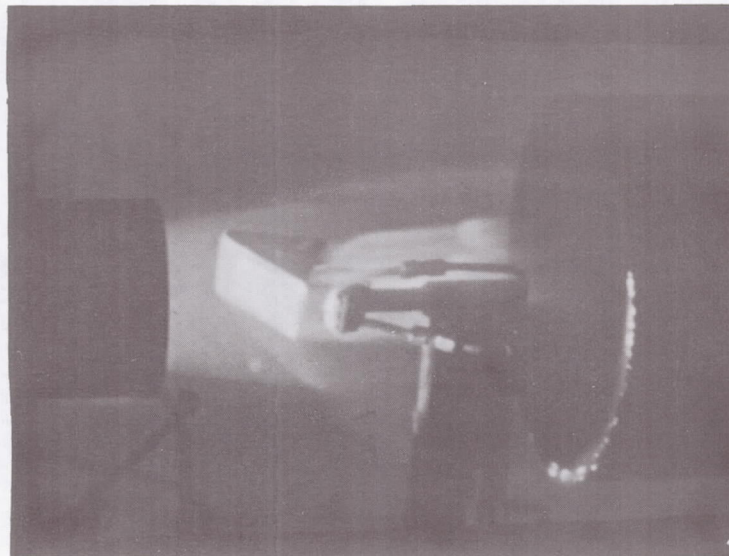
(b) High-heat-transfer condition. $\alpha = 0.49$ radian.   L-68-8518

Figure 8.- Photographs of 0.65-radian wedge model in stream with ablative panel in view.
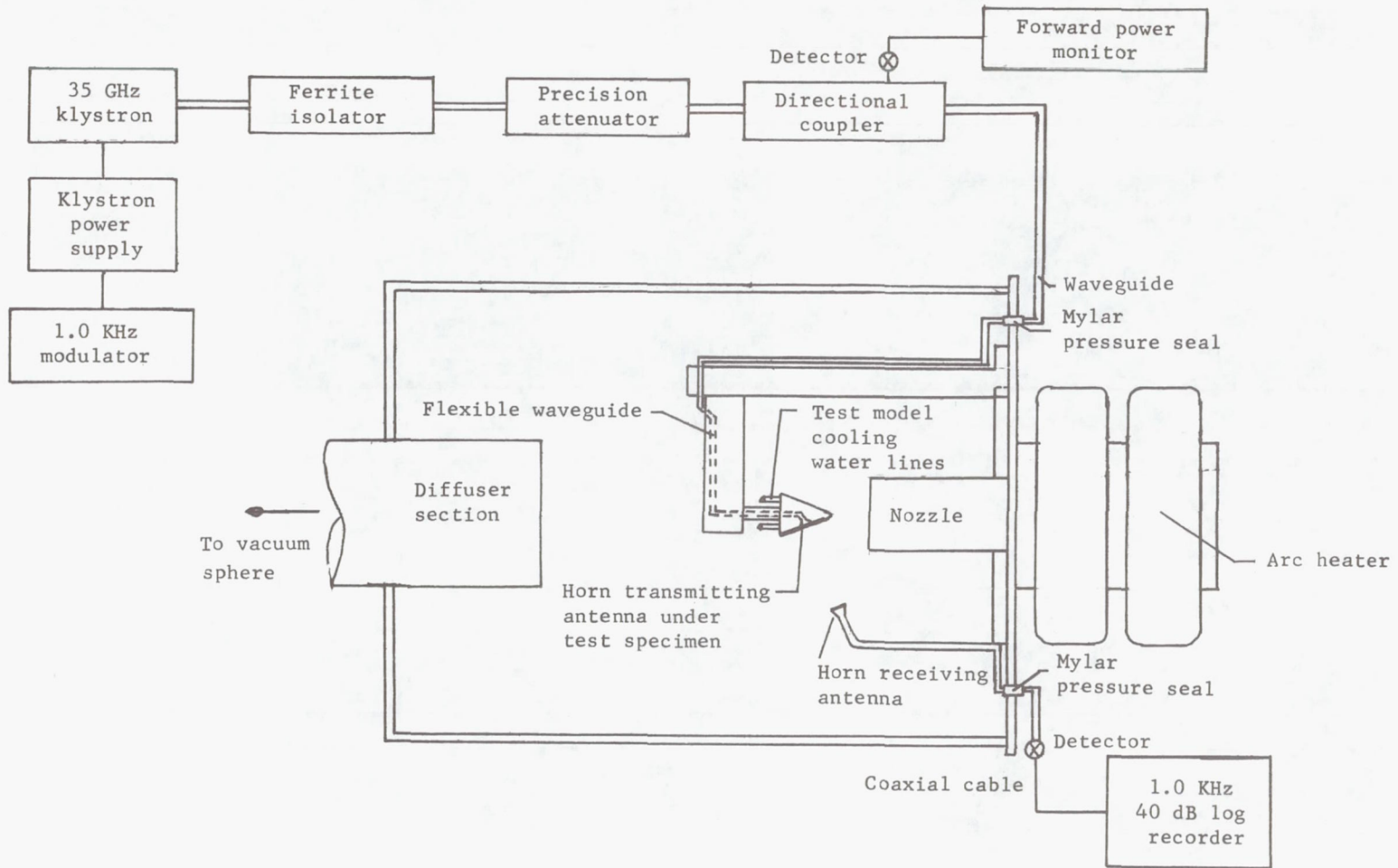
Figure 9.- Block diagram of instrumentation setup for transmission-loss measurements in arc tunnel.
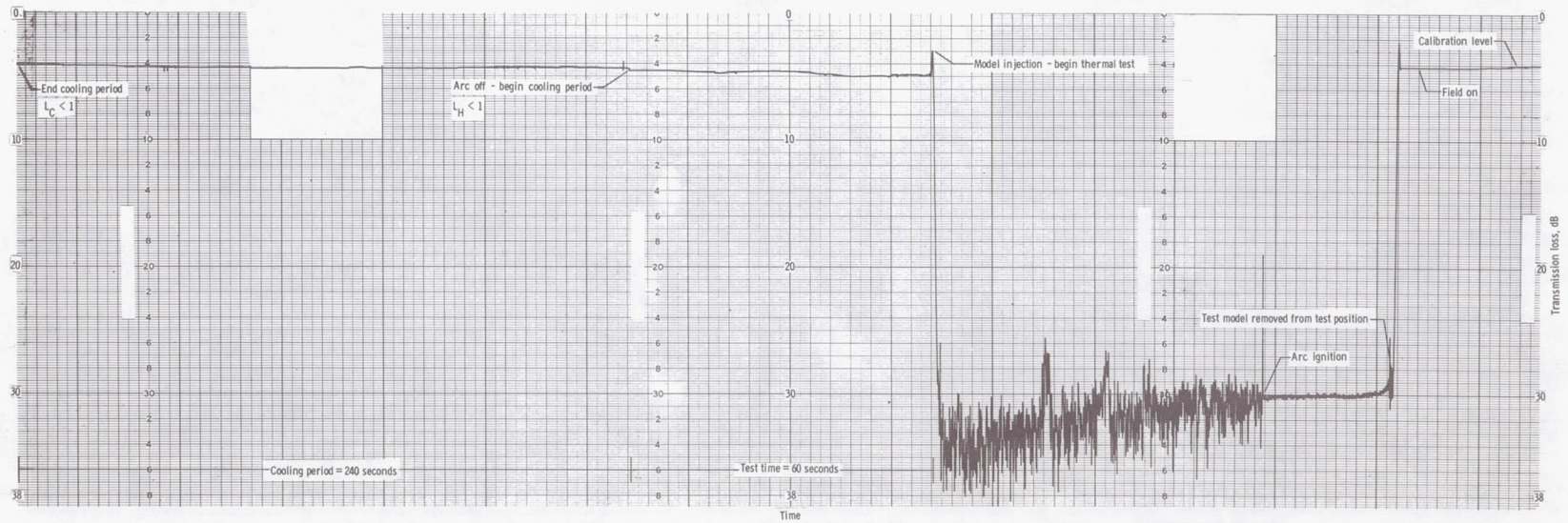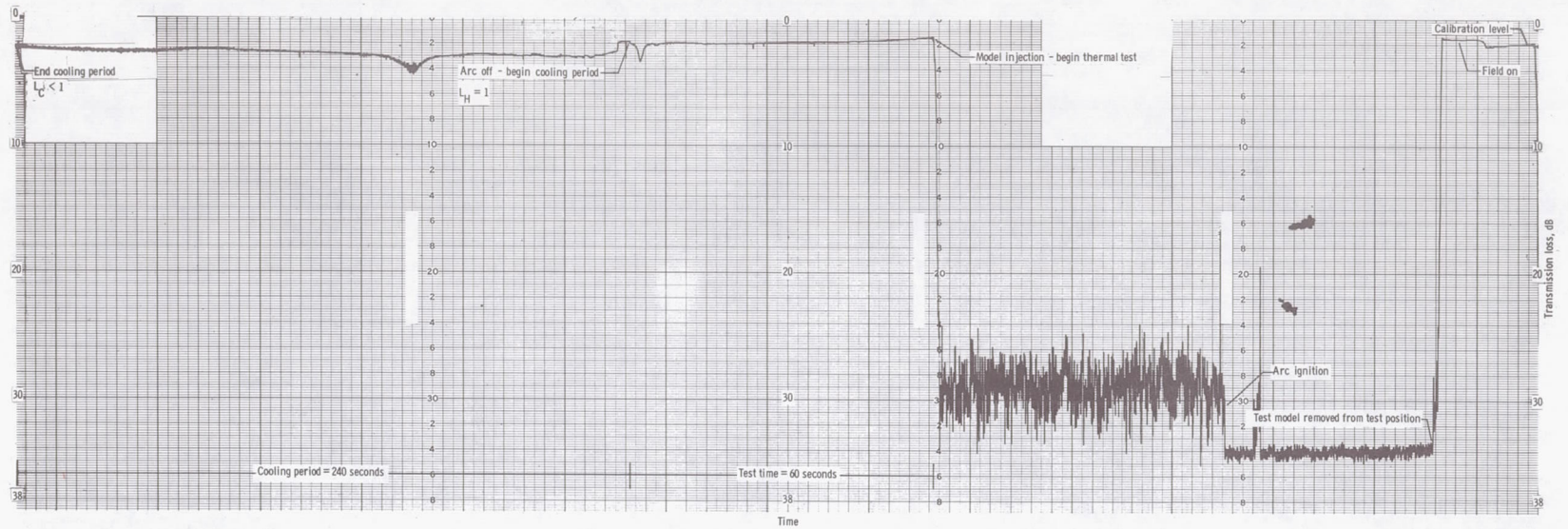
(a) Avco foamed teflon.

Figure 10.- Transmission loss recordings during low-heat-transfer ($\alpha = 0$ rad) test condition in arc tunnel.
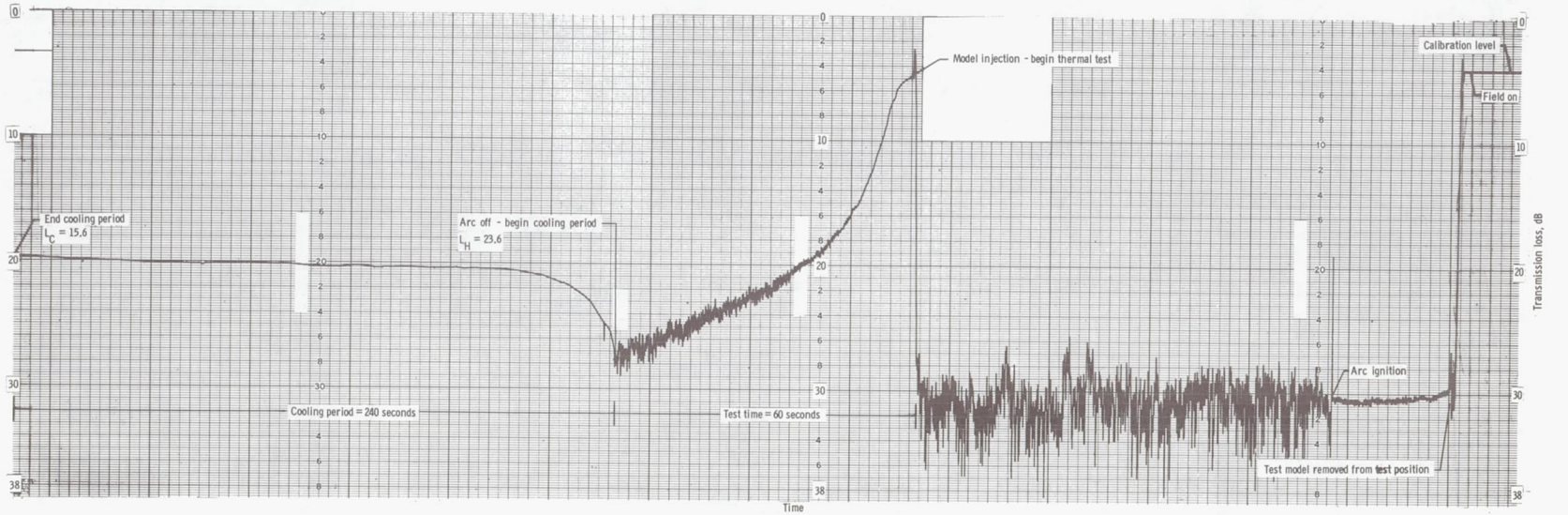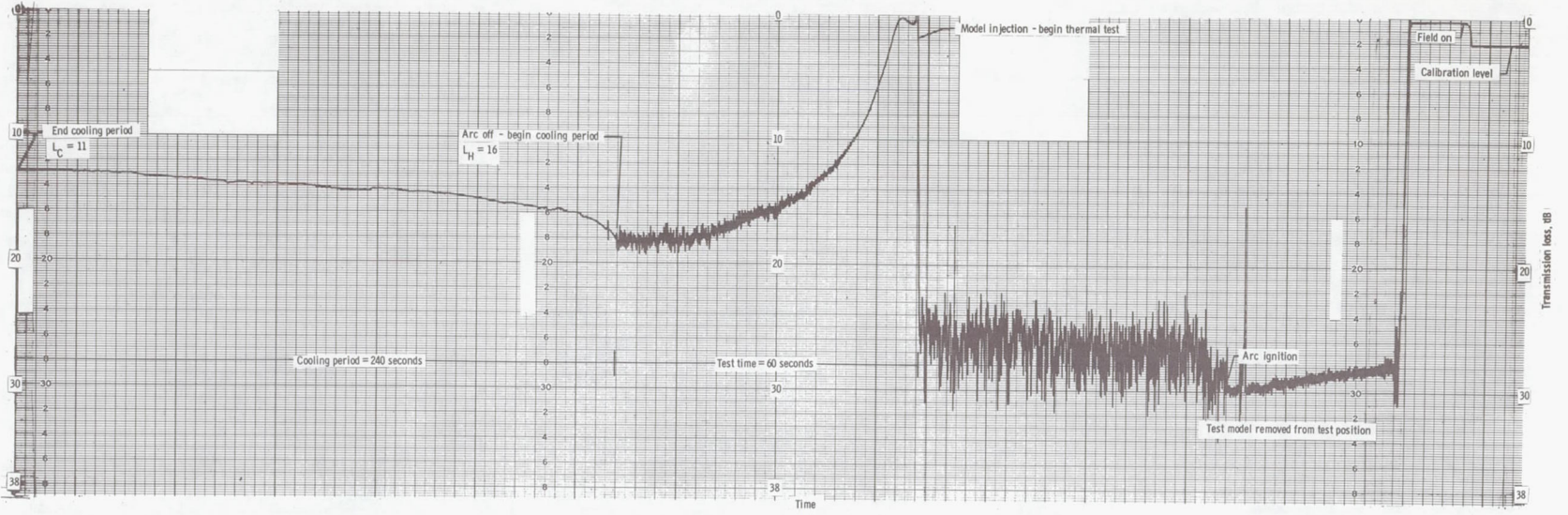
(b) Avco 893-23.

Figure 10.- Continued.
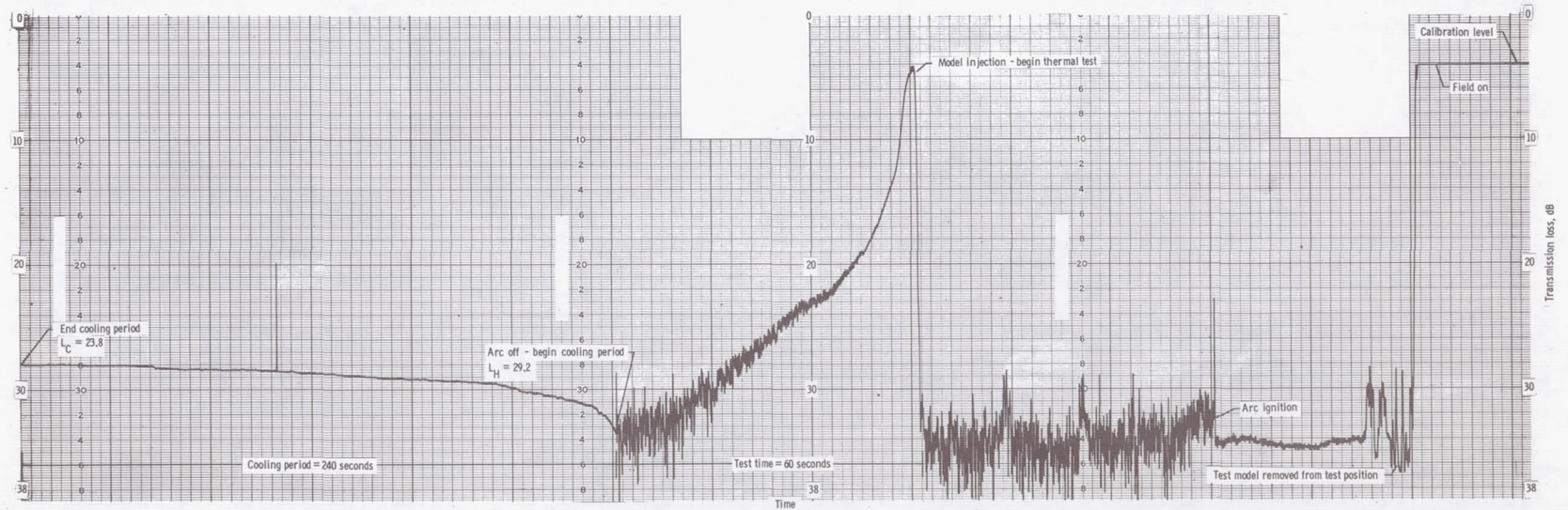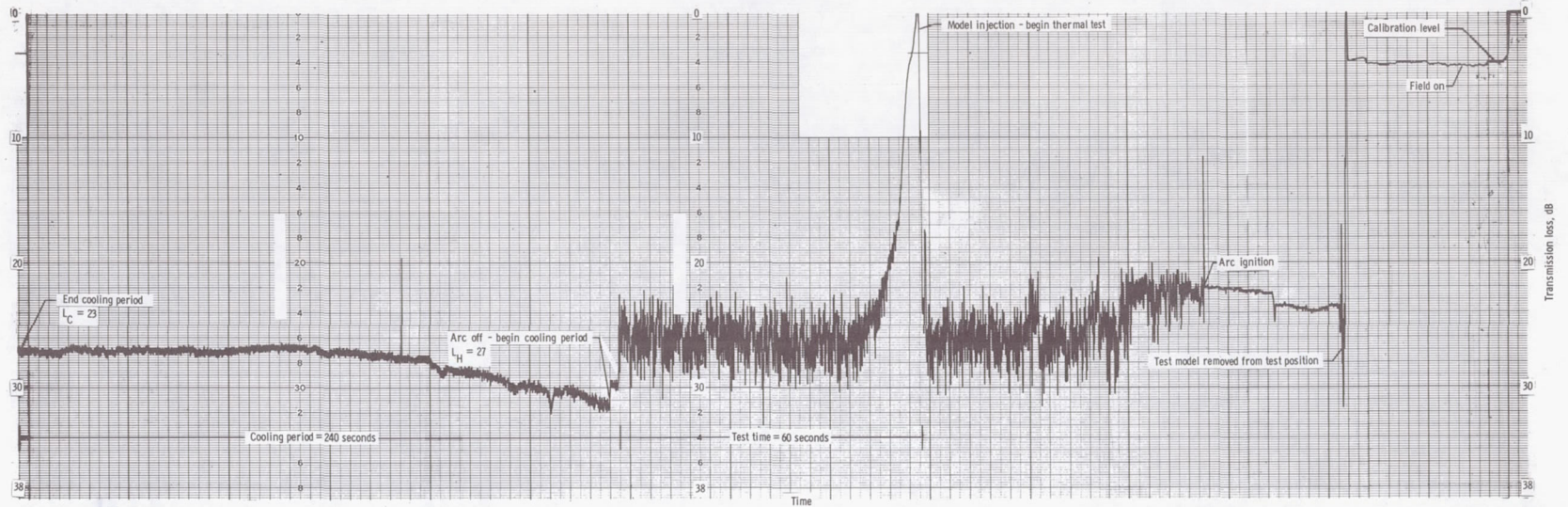
(c) Avcoat 5026-99A.

Figure 10.- Continued.
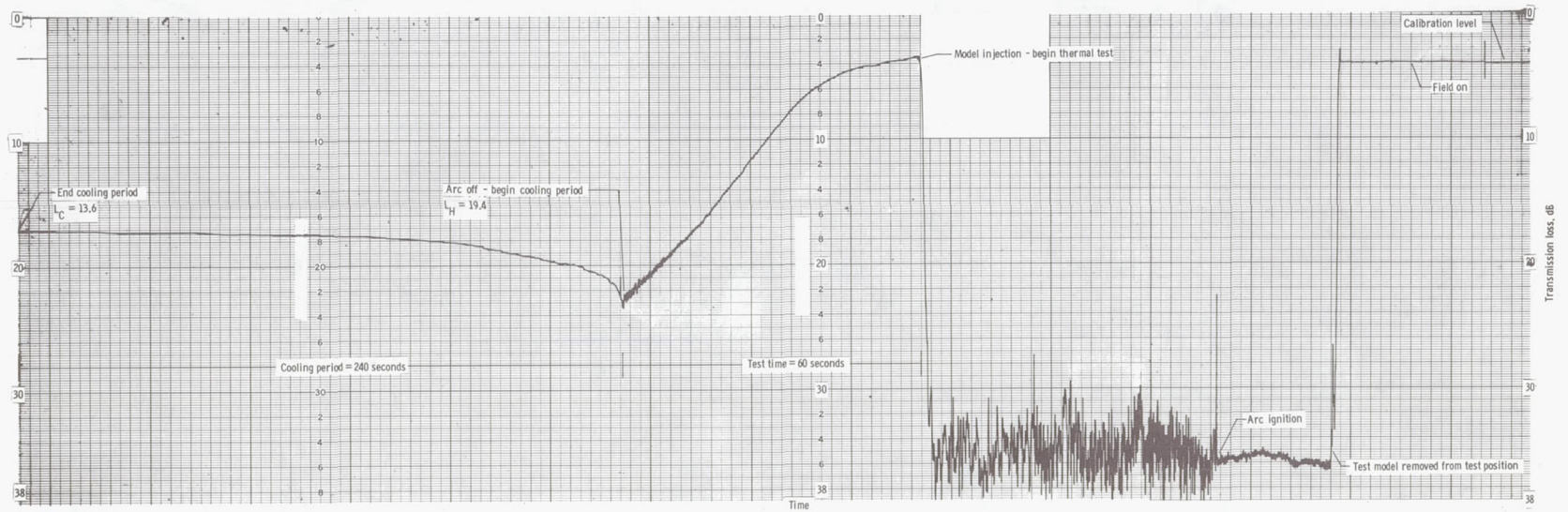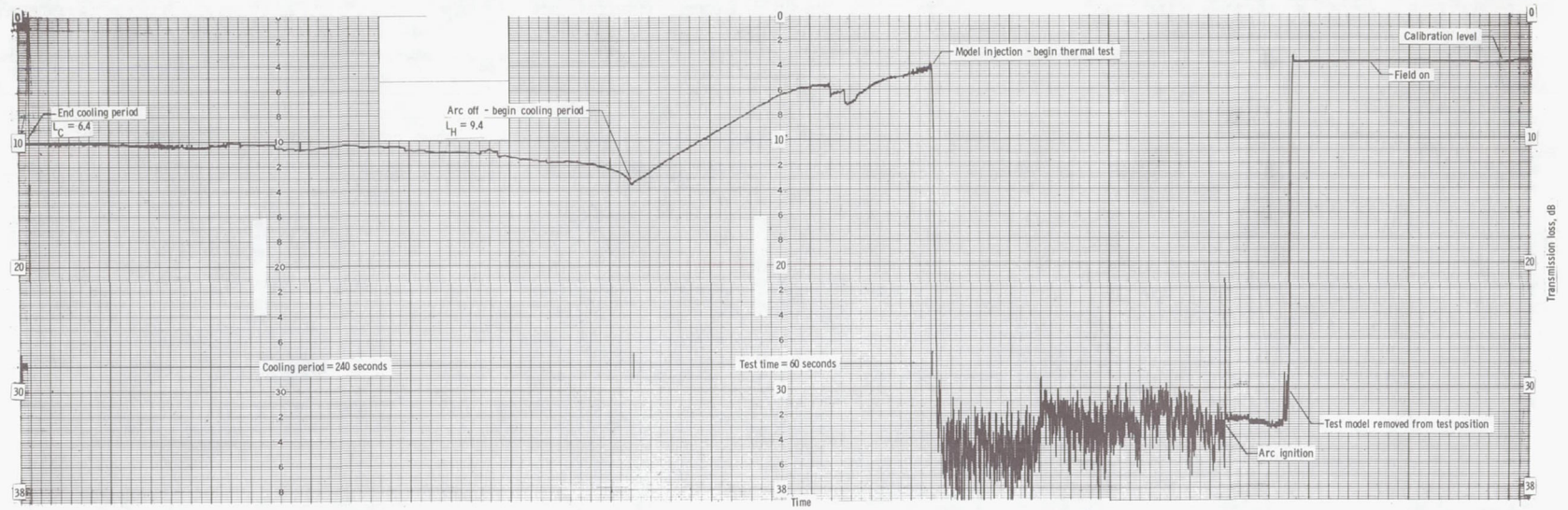
(d) Boeing poly carborazole.

Figure 10.- Continued.
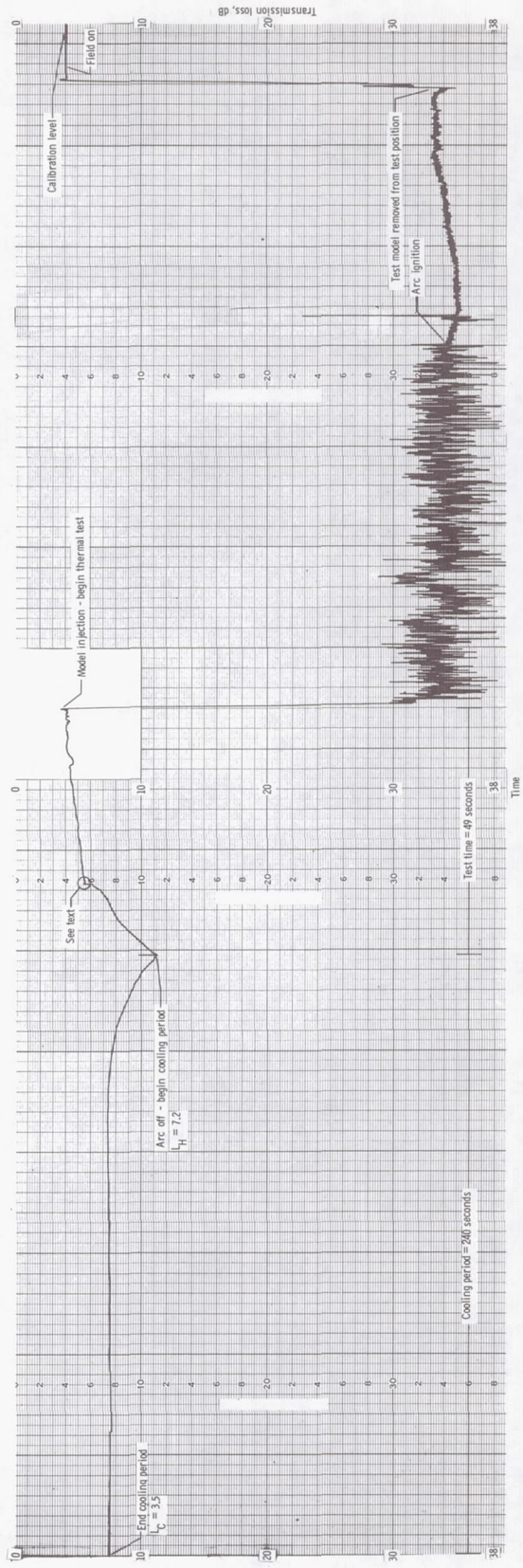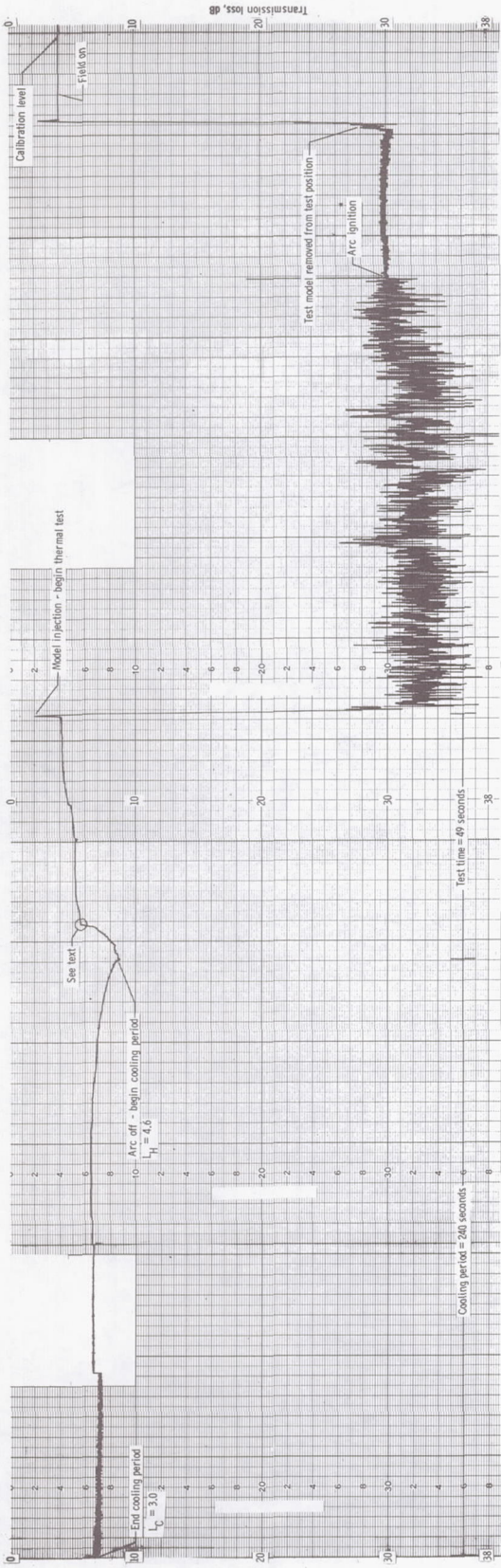
(e) McDonnell B47 RF.

Figure 10.- Continued.

End cooling period
$L_C < 1$

Arc off - begin cooling period
$L_H = 2.0$

Model injection - begin thermal test

Calibration level

Field on

Cooling period = 240 seconds

Test time = 60 seconds

Test model removed from test position

Arc ignition

Transmission loss, dB

End cooling period
$L_C < 1$

Arc off - begin cooling period
$L_H = 1.9$

Model injection - begin thermal test

Calibration level

Field on

Cooling period = 240 seconds

Test time = 60 seconds

Test model removed from test position

Arc ignition

Transmission loss, dB

(f) Martin SLA-220.

Figure 10.- Continued.
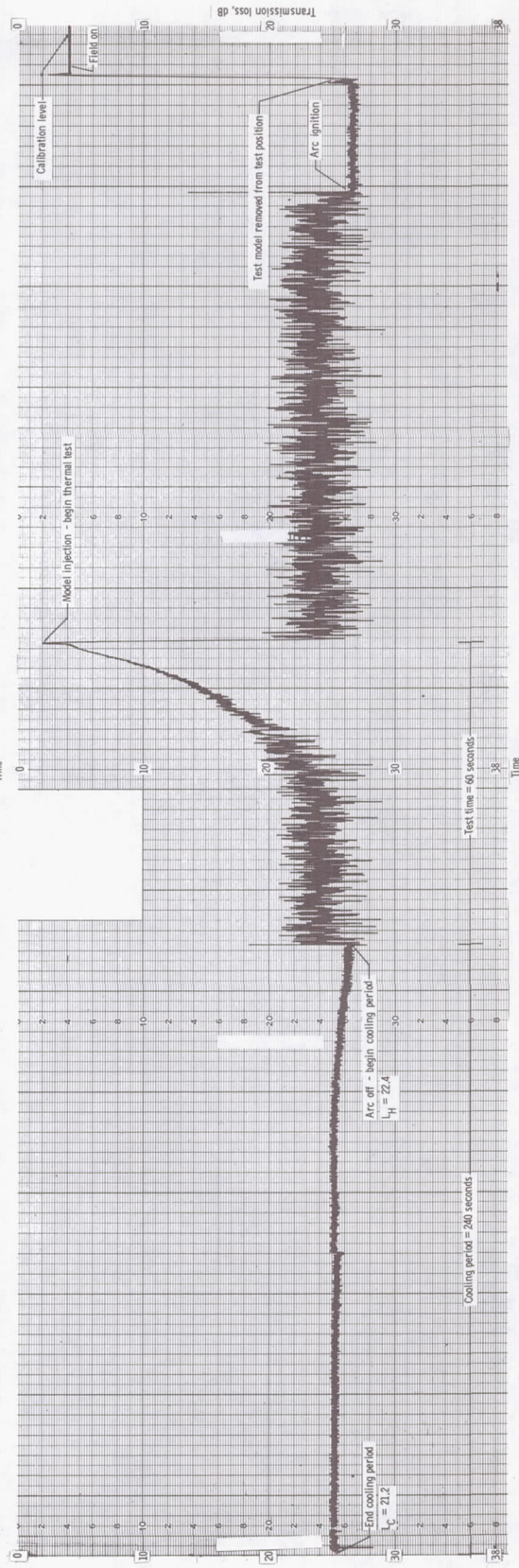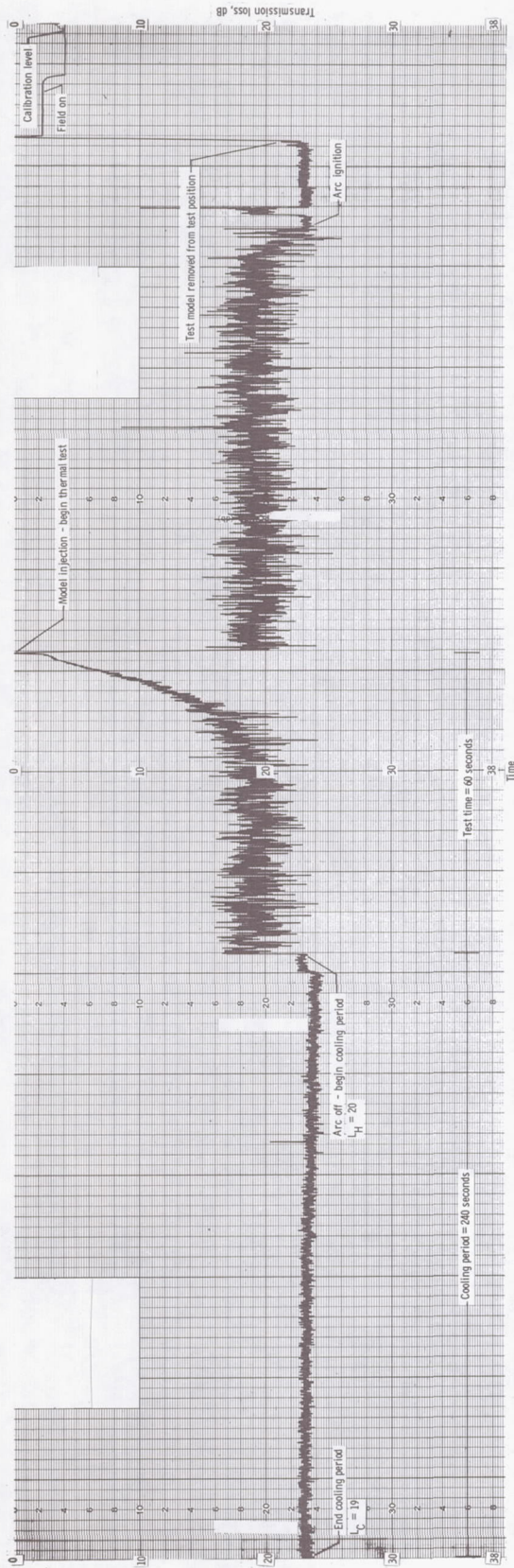
(g) Martin SLA-561.

Figure 10.- Continued.
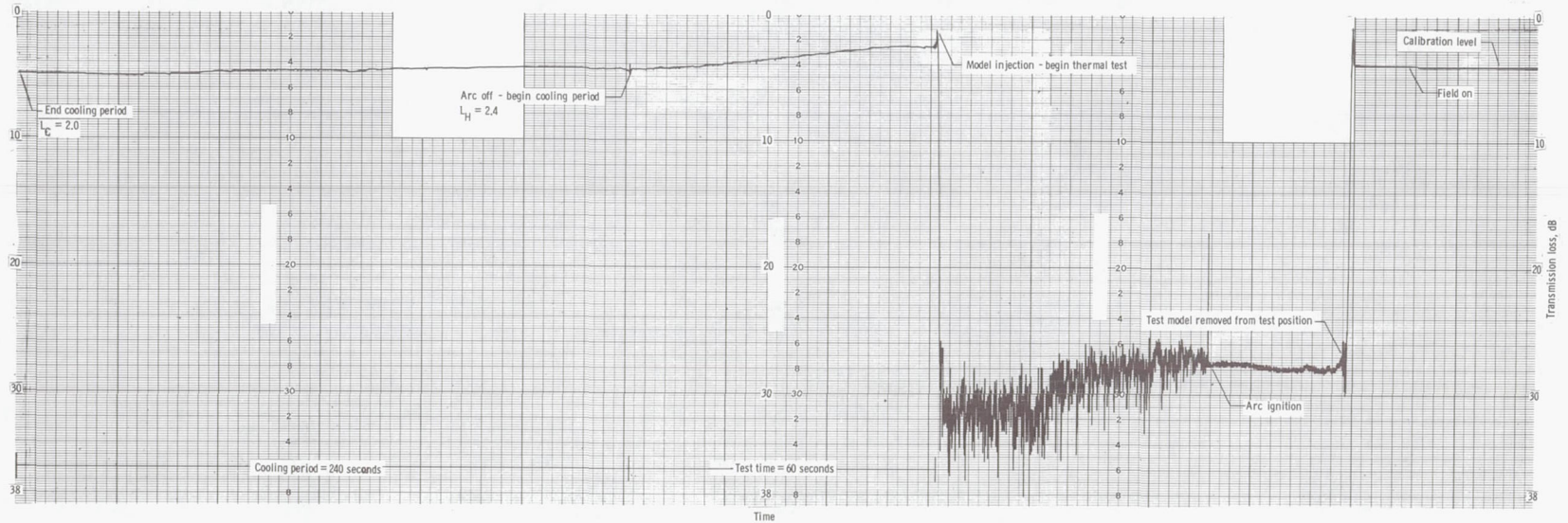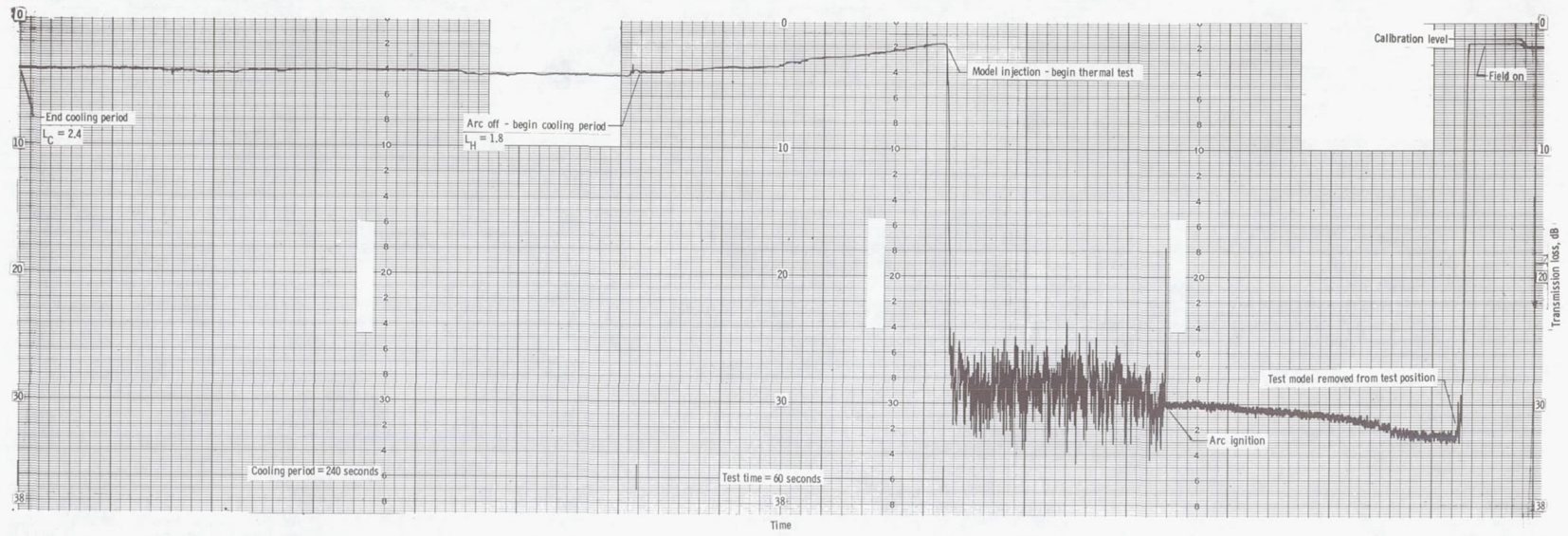
(h) E4A1.

Figure 10.- Continued.
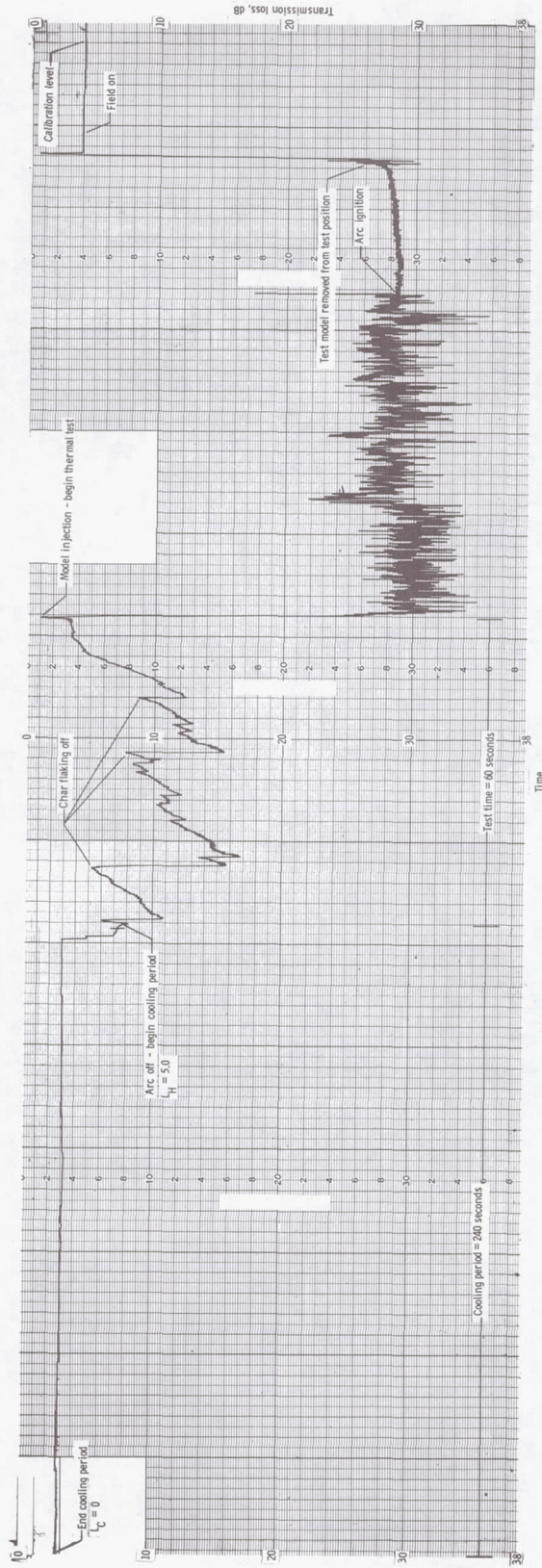
(i) E6A7.

Figure 10.- Concluded.
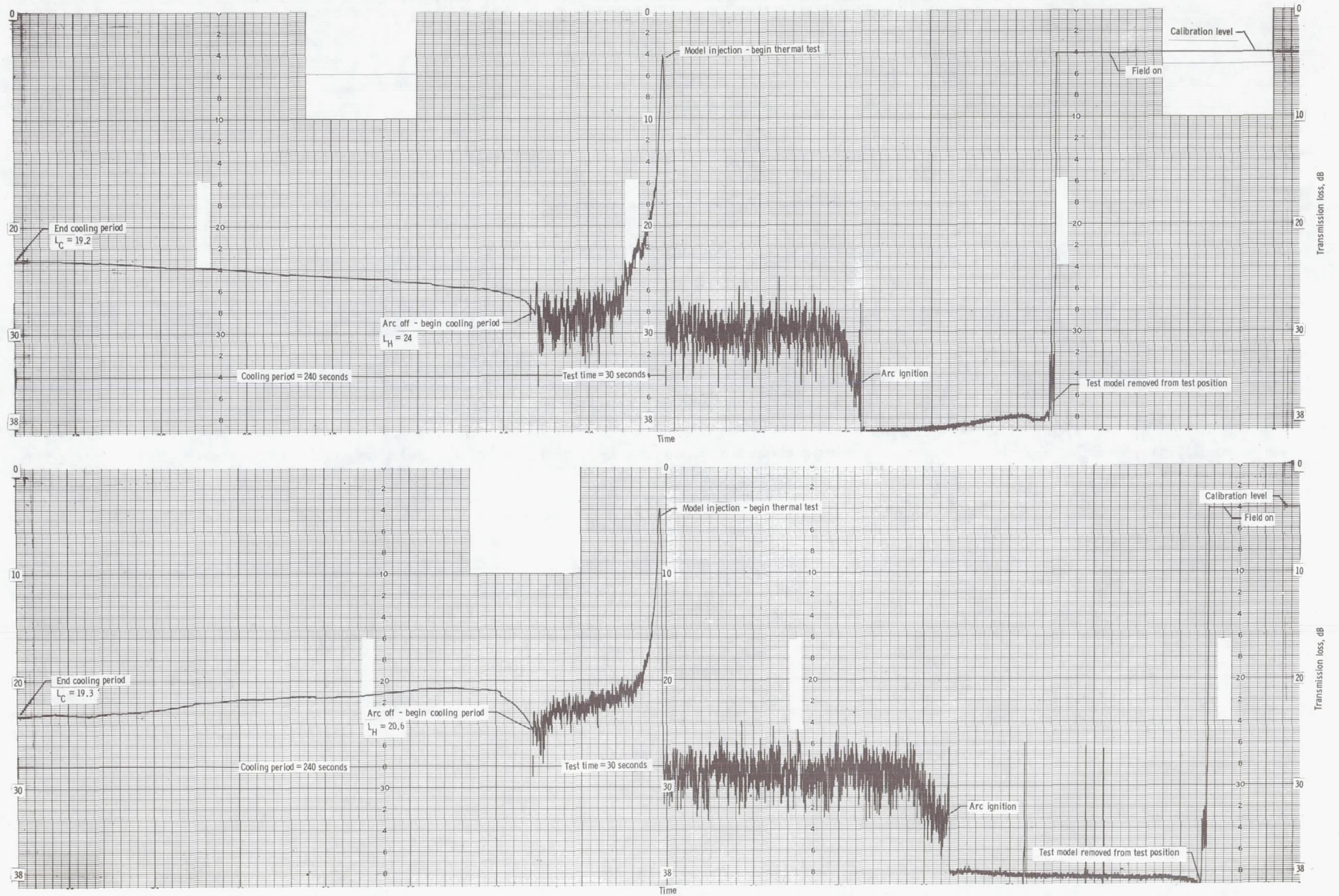
(a) Avco 893-23.

Figure 11.- Transmission loss recordings during high-heat-transfer (α = 0.49 radian) test condition in arc tunnel.
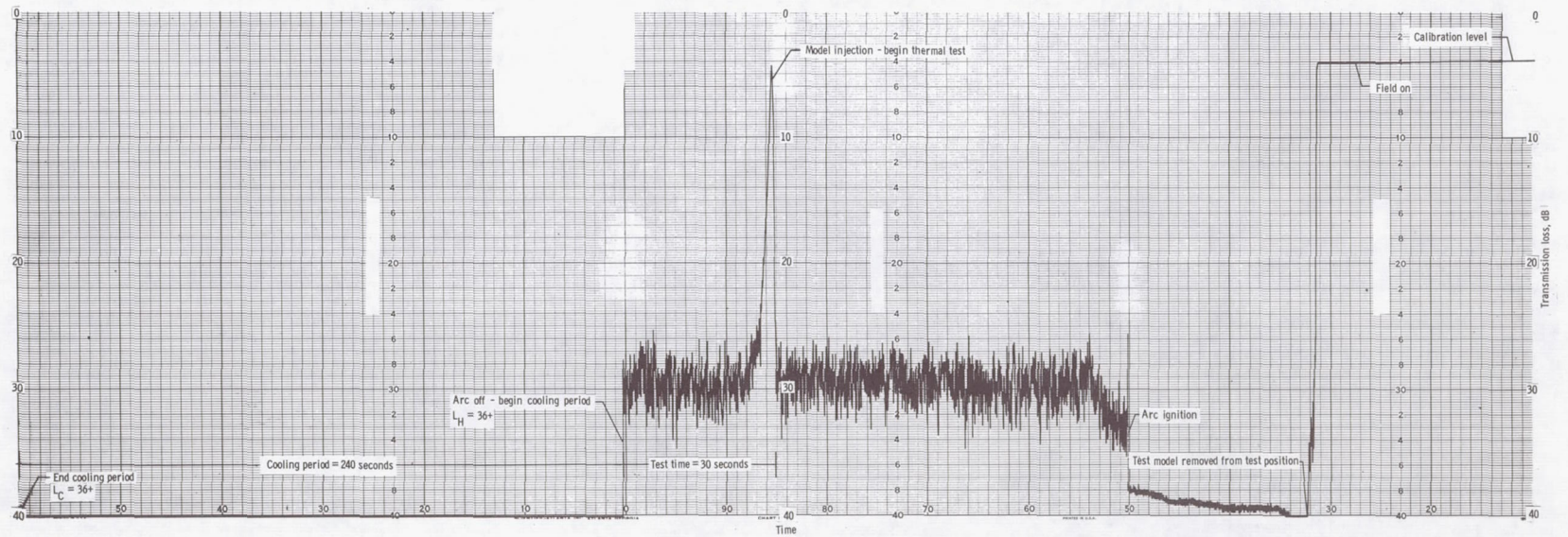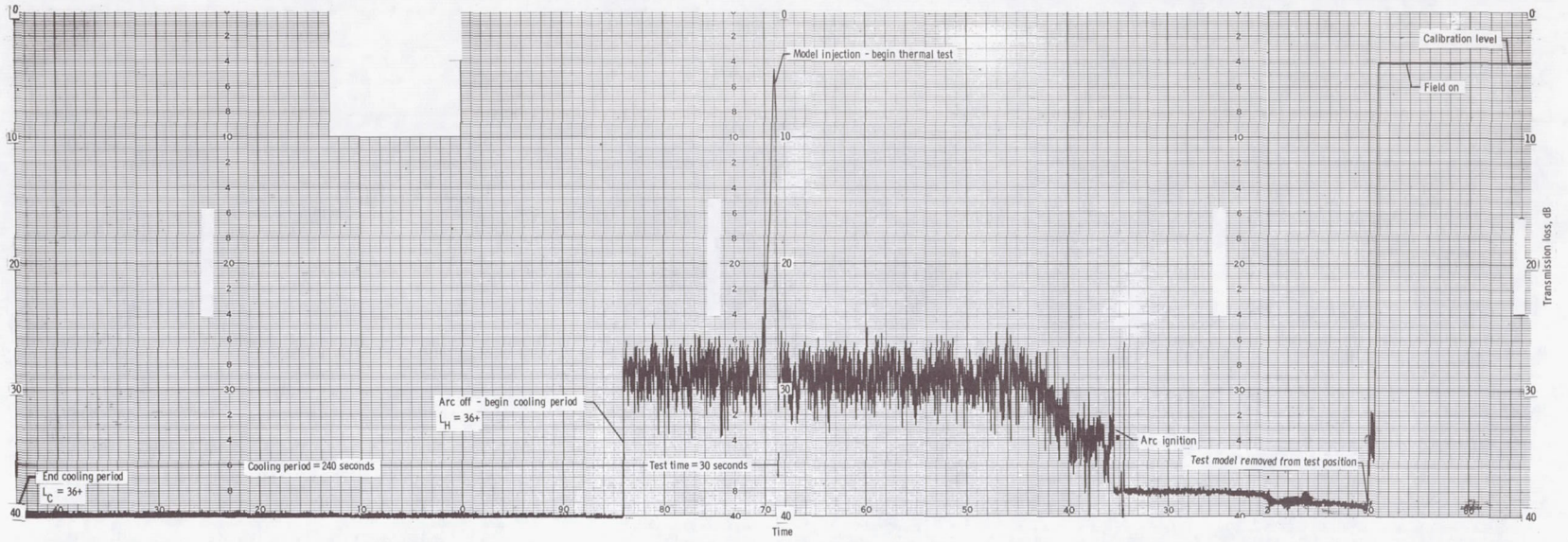
(b) Avcoat 5026-99A.

Figure 11.- Continued.
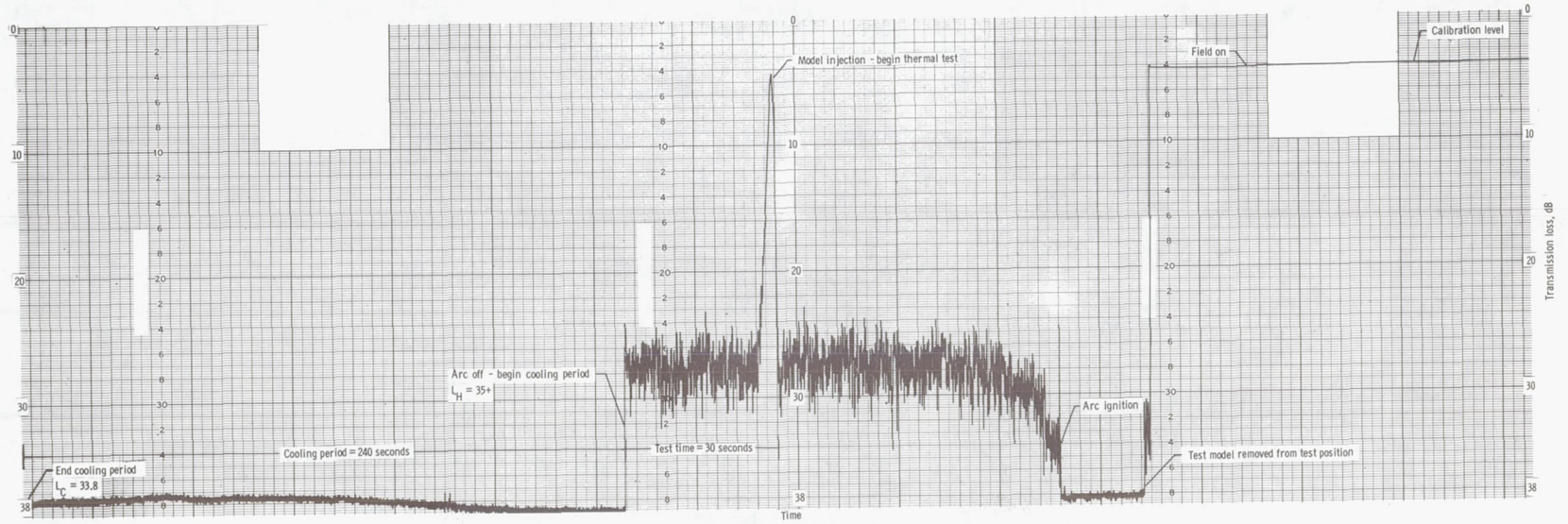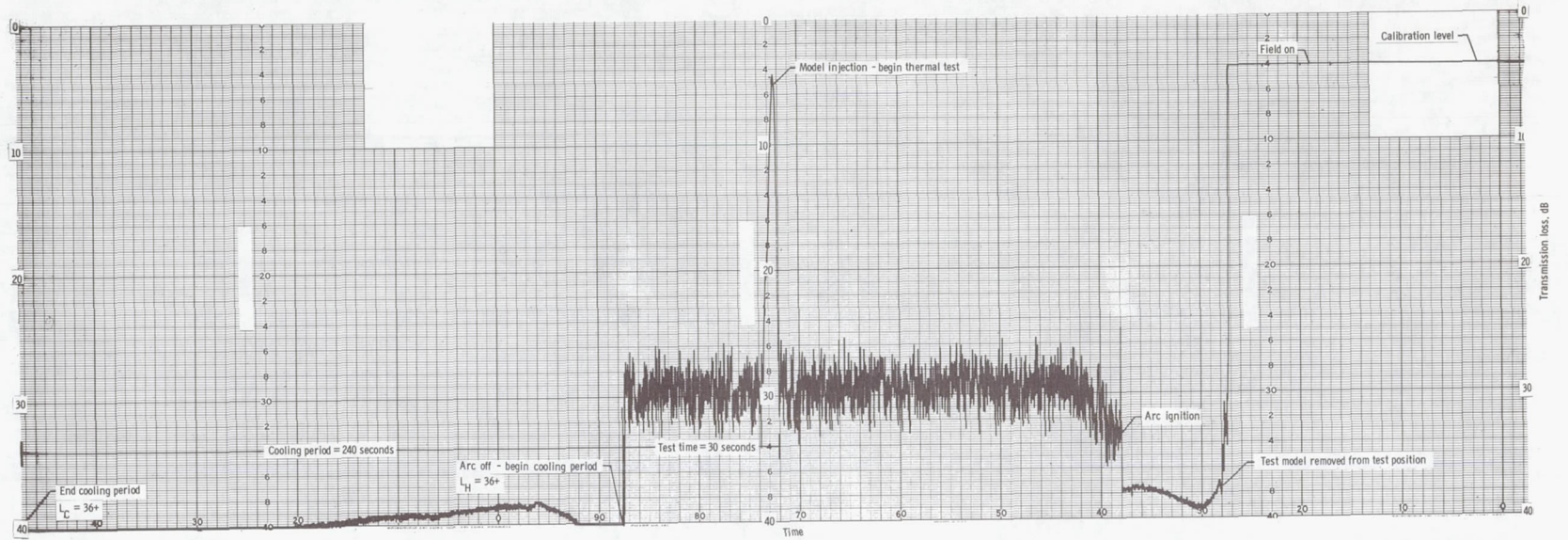
(c) Avcoat 5026-39 HCG.

Figure 11.- Continued.
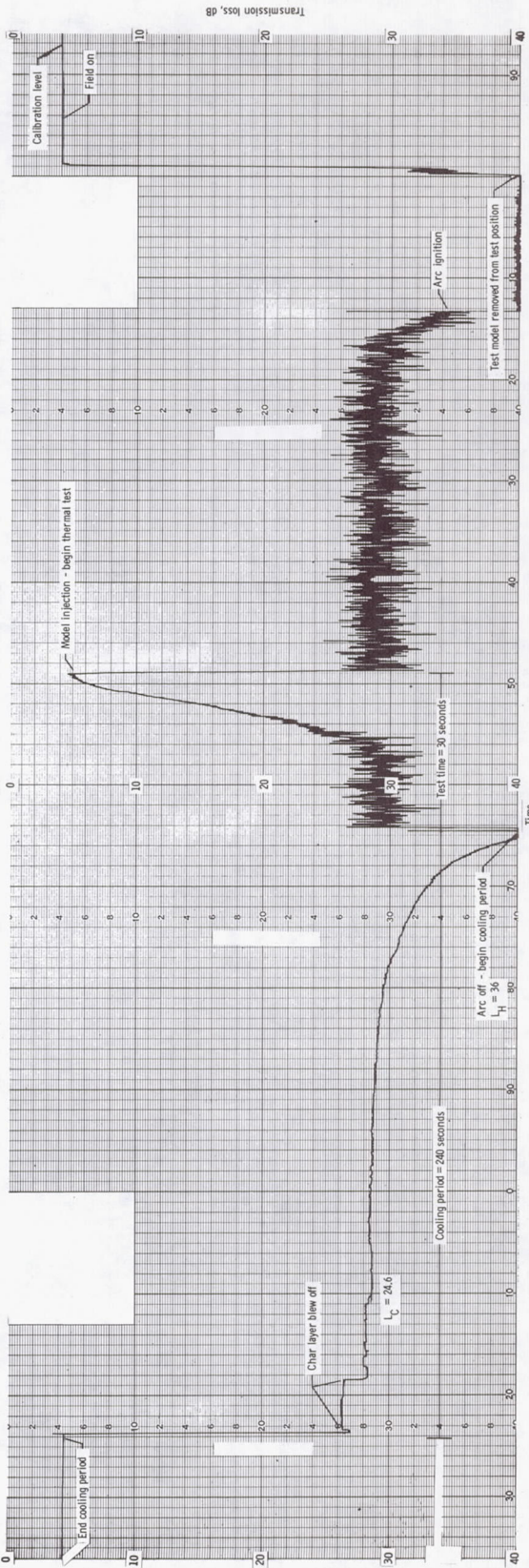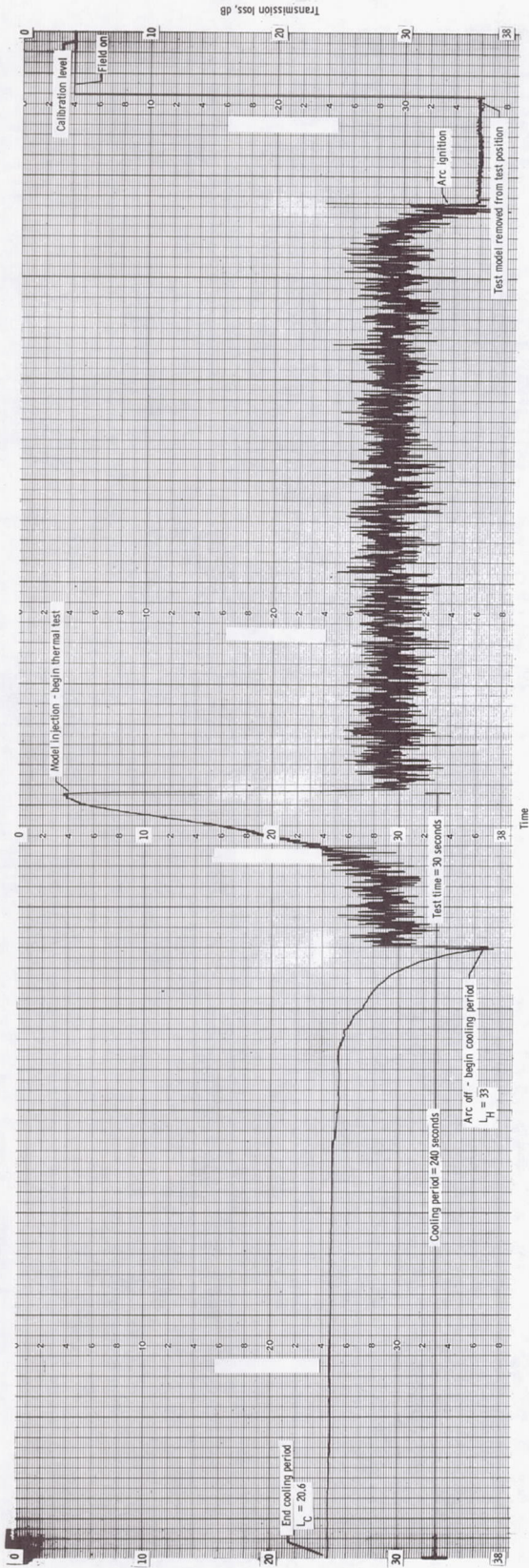
(d) Avco Mod 7.

Figure 11.- Continued.
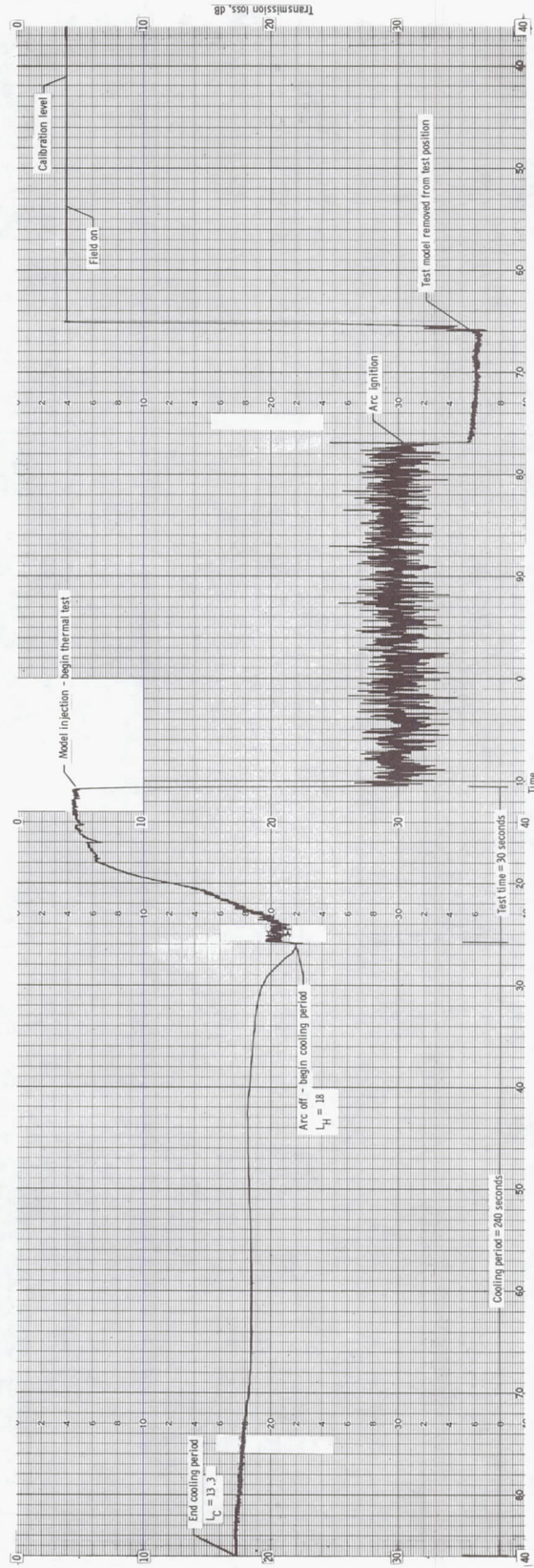
(e) Boeing poly carborazole.

Figure 11.- Continued.
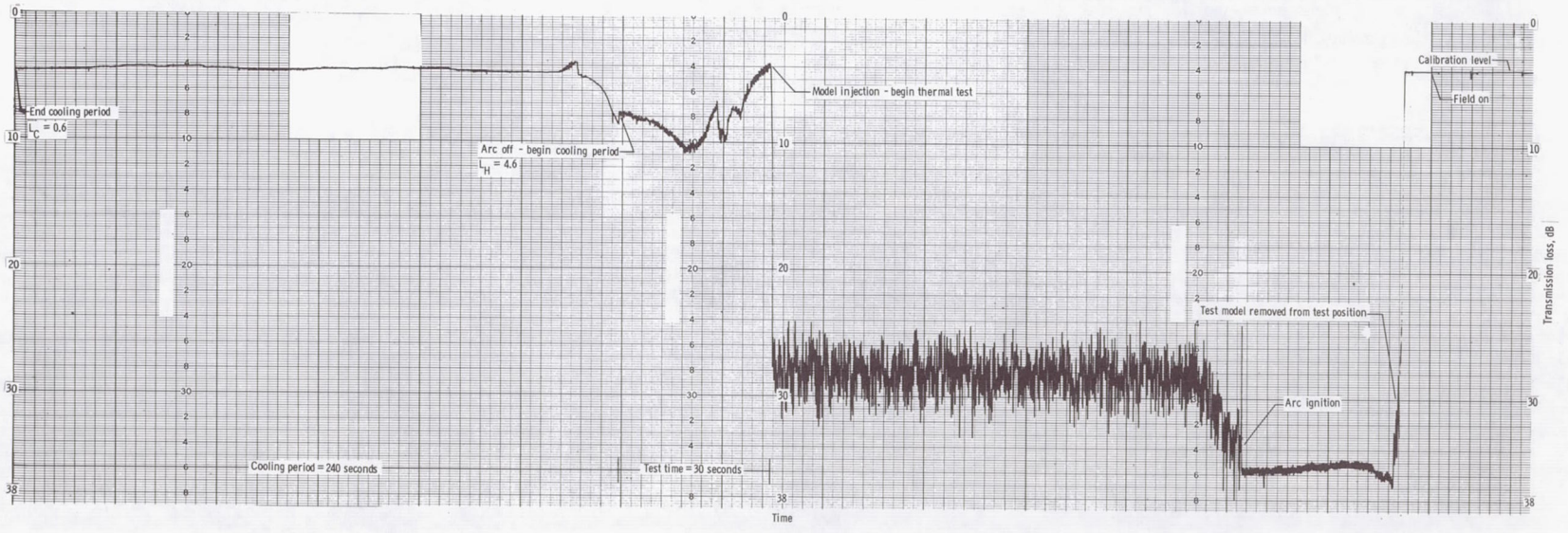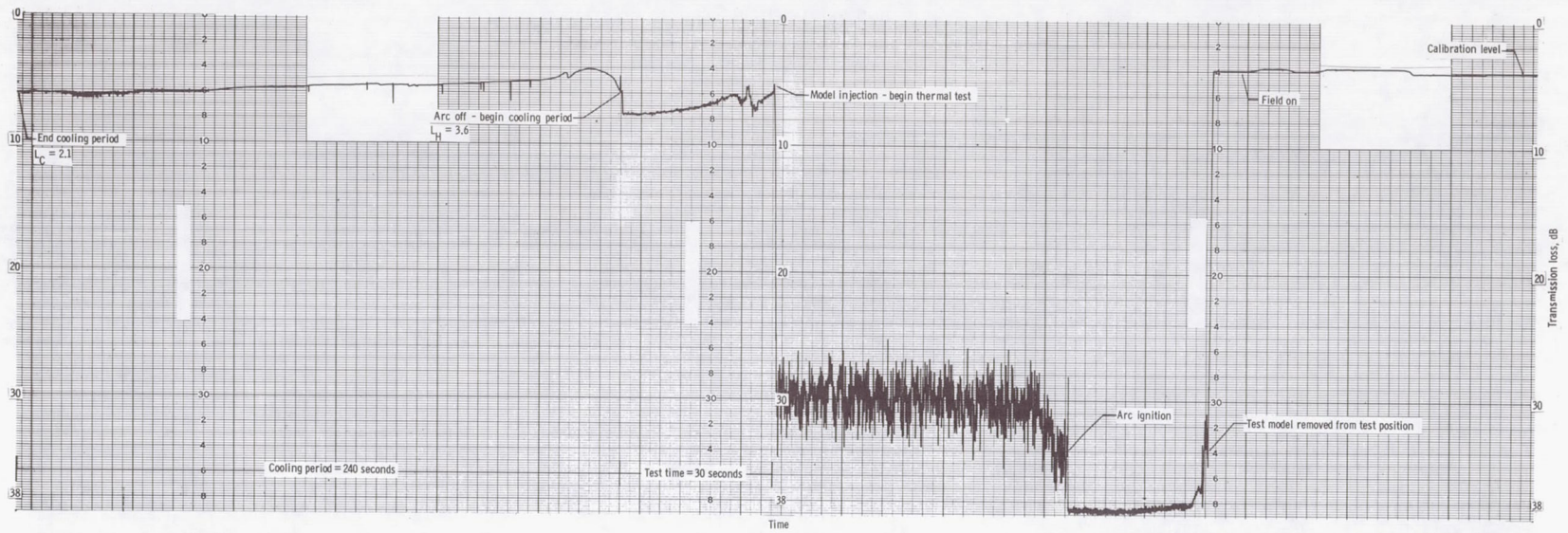
(f) Martin SLA-220.

Figure 11.- Continued.
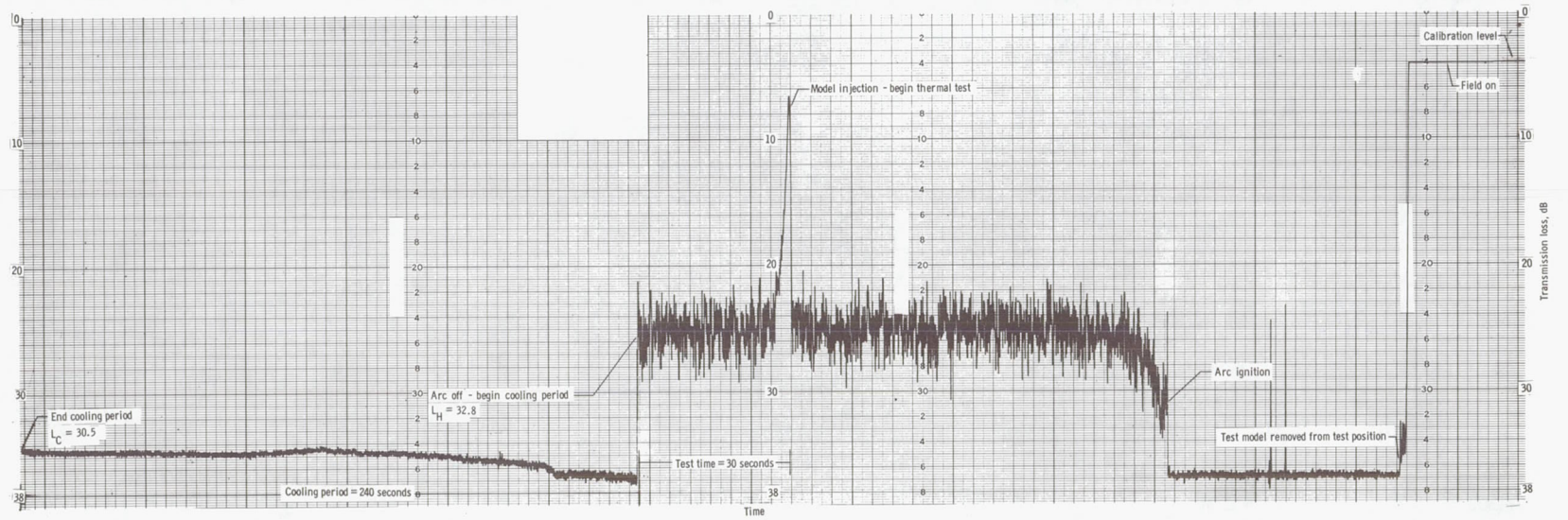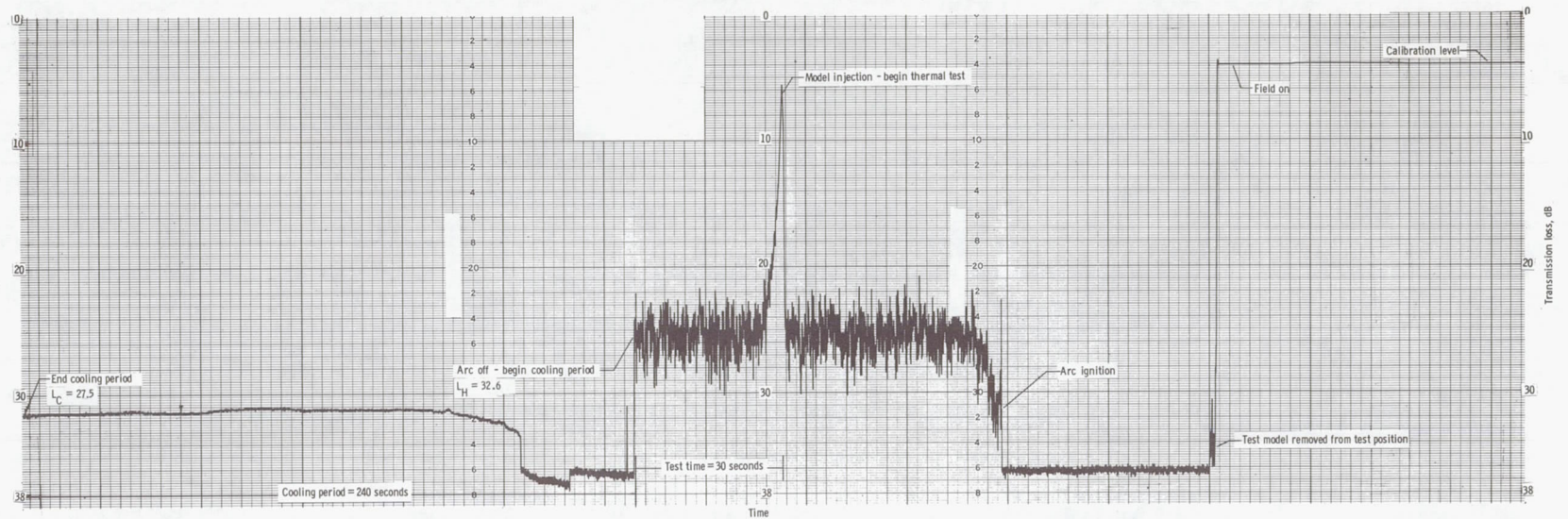
(g) Martin SLA-561.

Figure 11.- Continued.
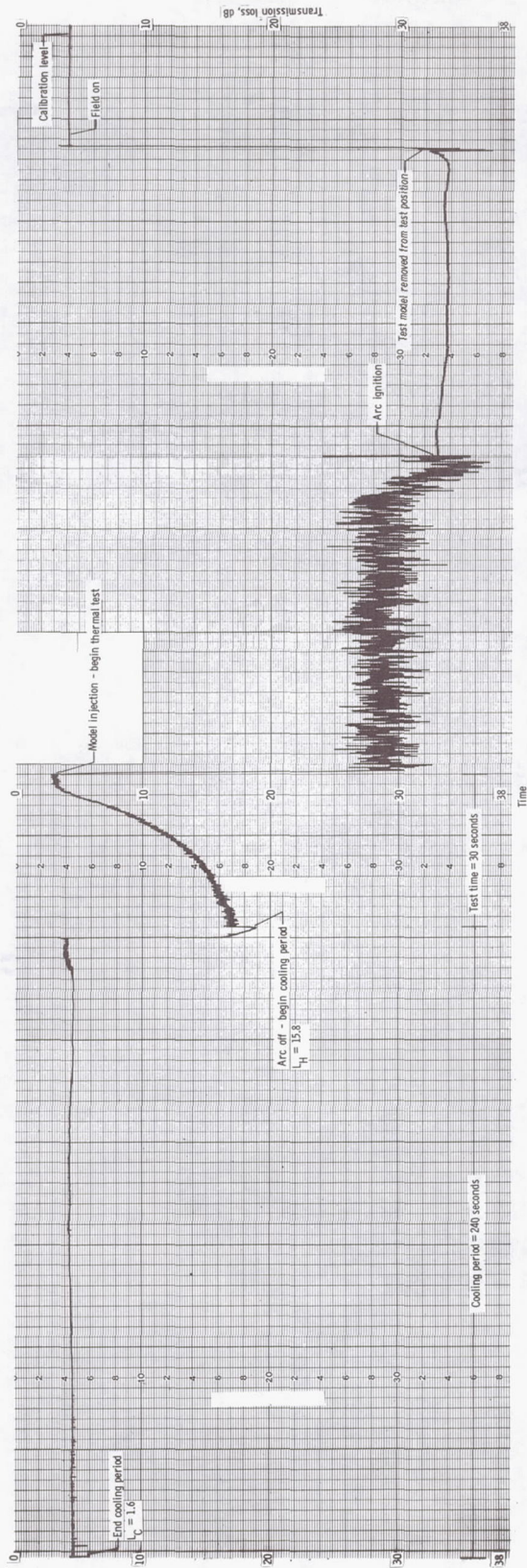
(h) E4A1.

Figure 11.- Concluded.
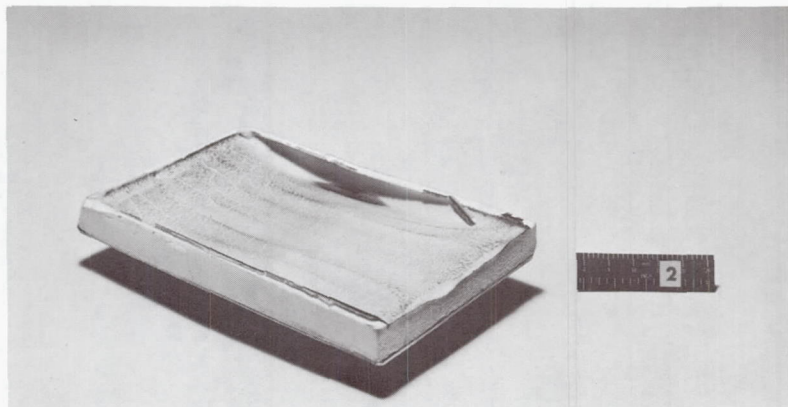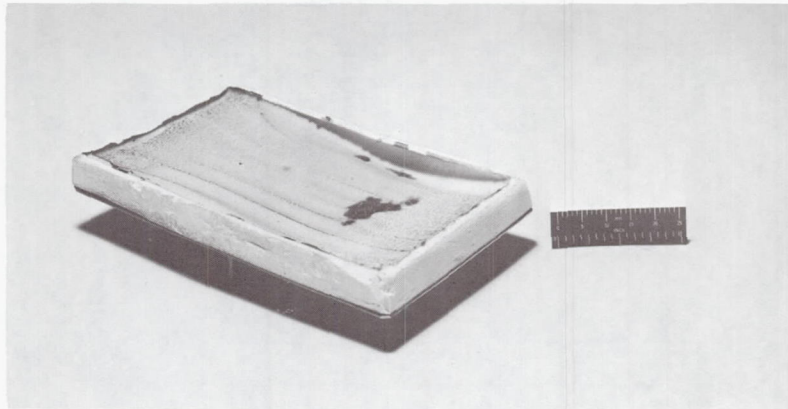
(a) Avco foamed teflon.   L-68-8519

Figure 12.- Photographs of test specimens before and after exposure to low-heat-transfer ($\alpha = 0$ rad) test condition in arc tunnel.
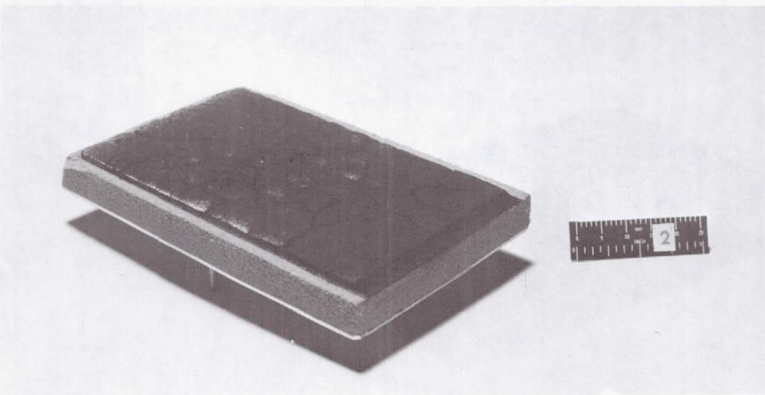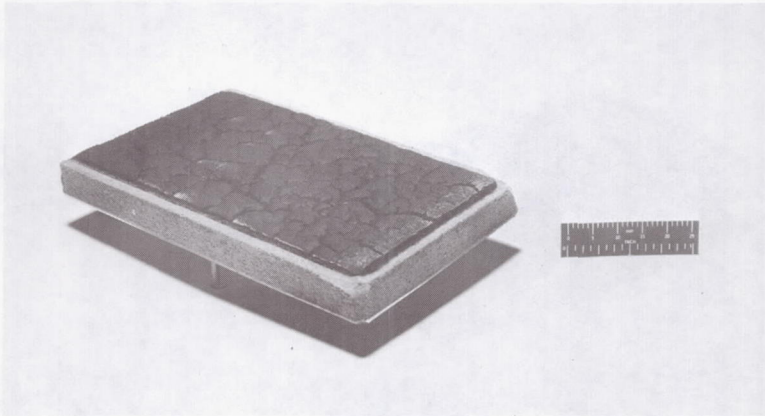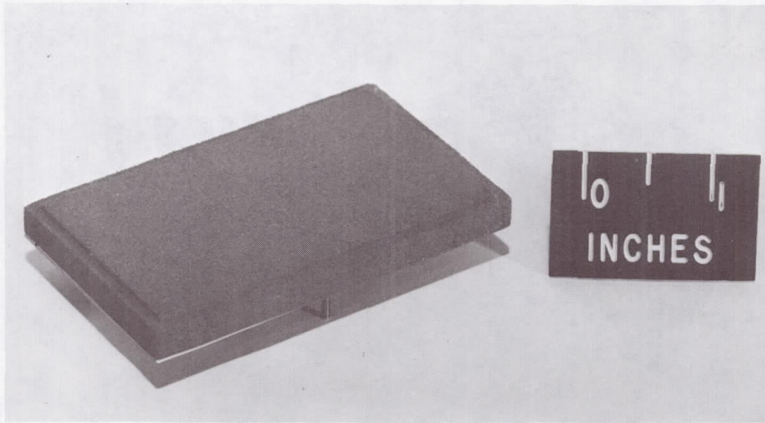
(b) Avco 893-23.   L-68-8520

Figure 12.- Continued.
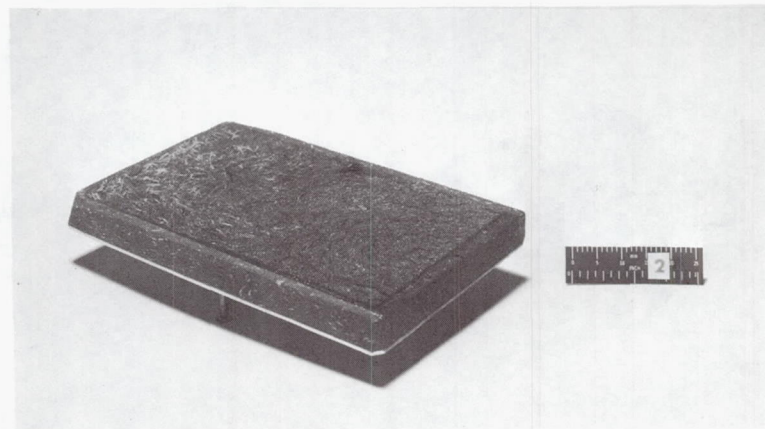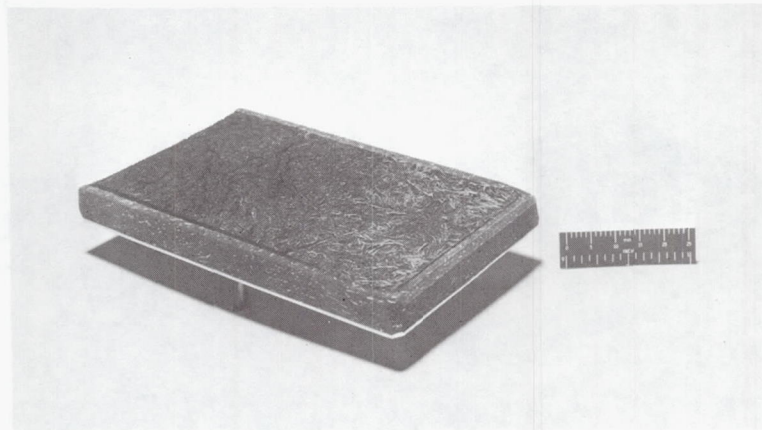
(c) Avcoat 5026-99A.   L-68-8521

Figure 12.- Continued.
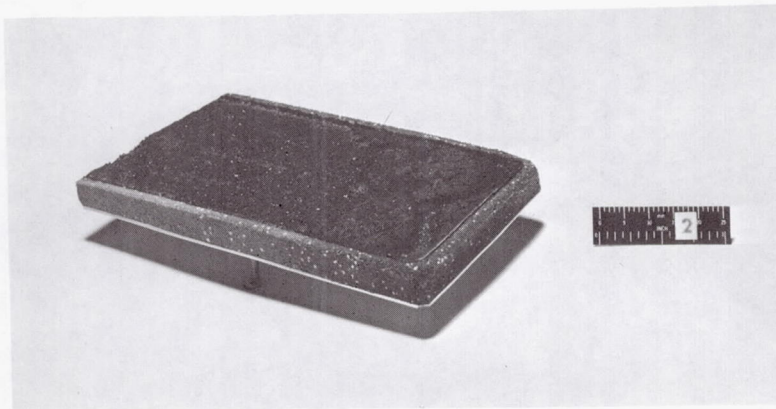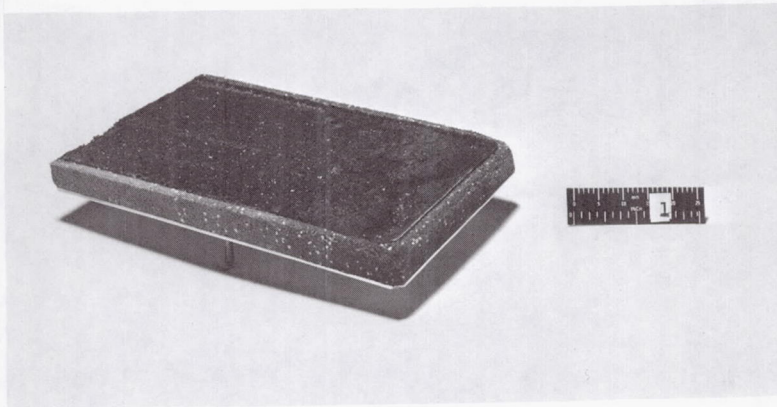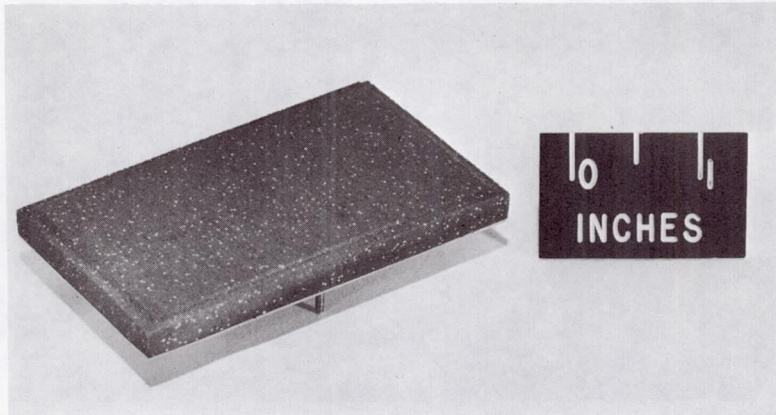
(d) Boeing poly carborazole.   L-68-8522

Figure 12.- Continued.
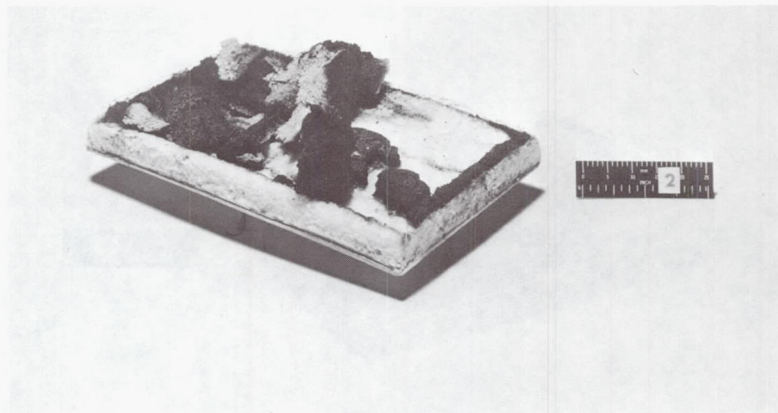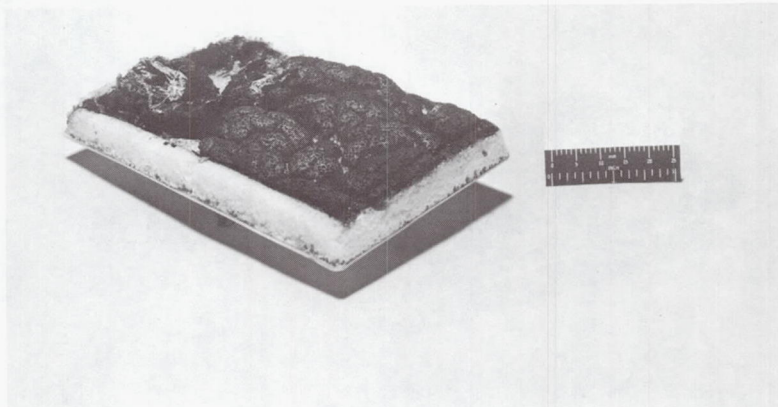
(e) McDonnell B47 RF.   L-68-8523
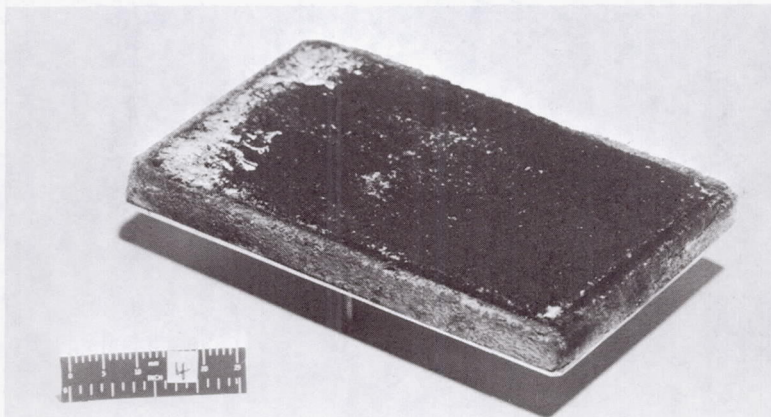
Figure 12.- Continued.
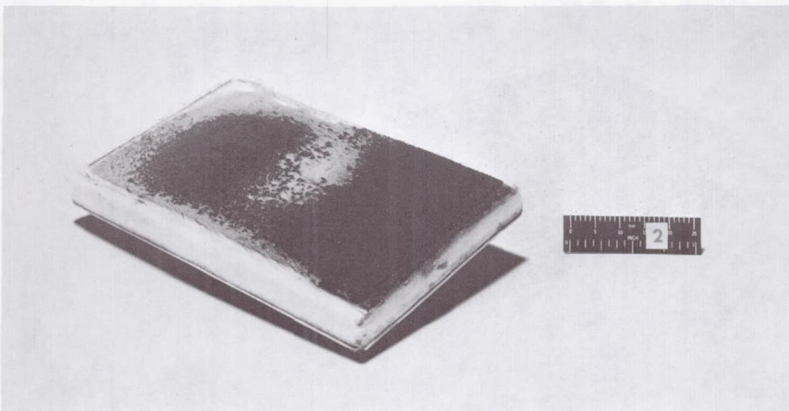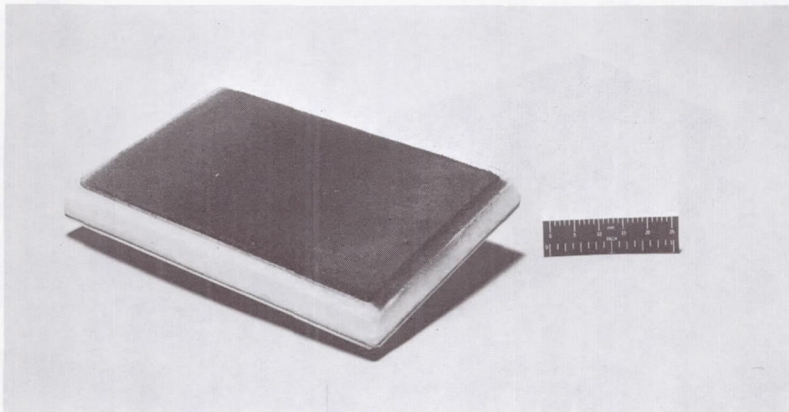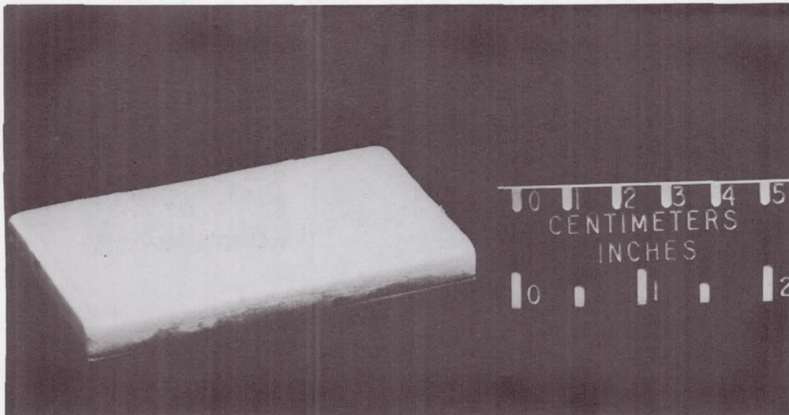
(f) Martin SLA-220.   L-68-8524

Figure 12.- Continued.
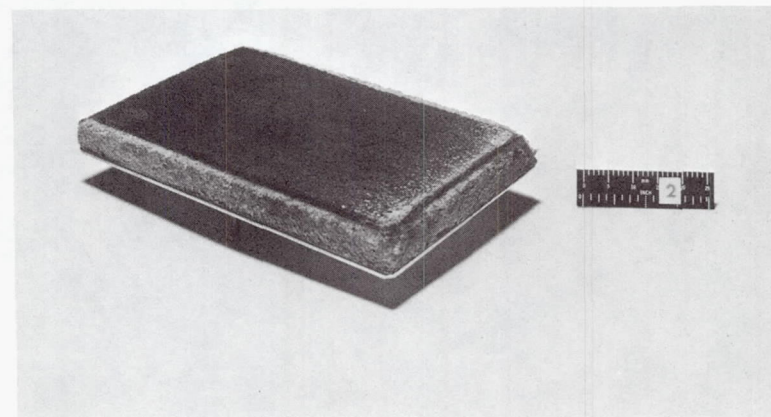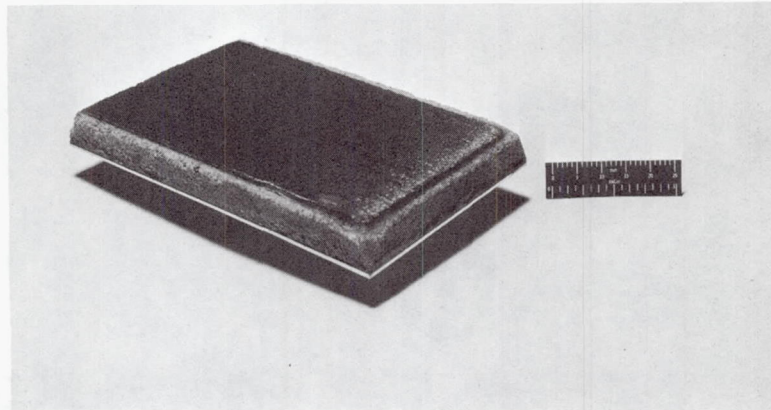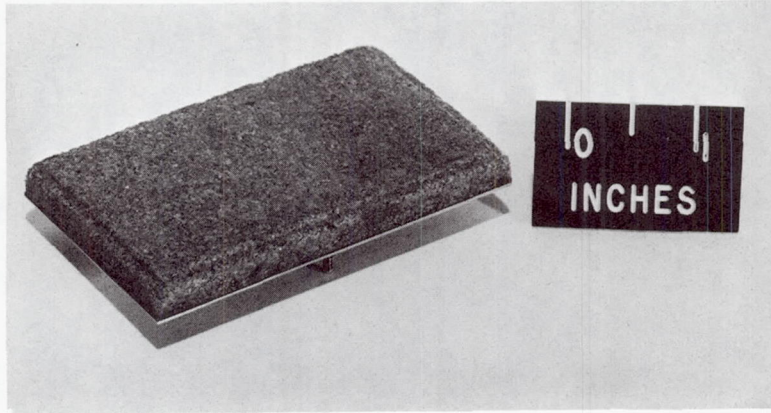
(g) Martin SLA-561.   L-68-8525

Figure 12.- Continued.
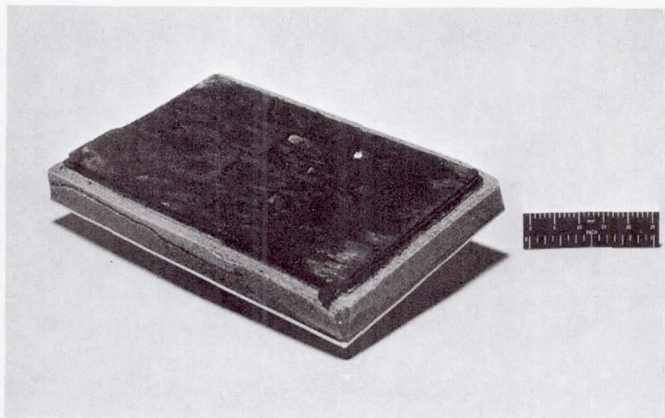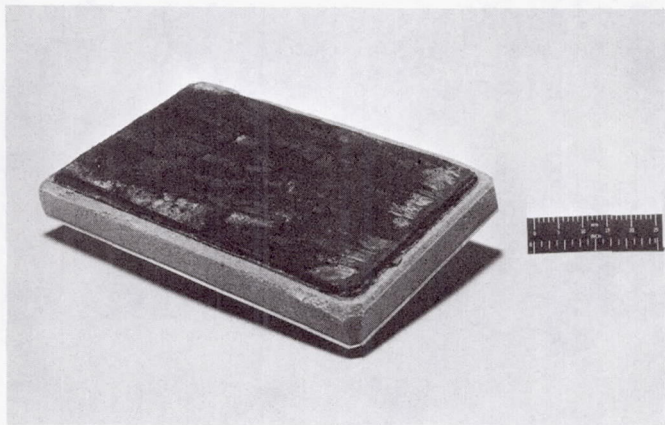
(h) E4A1.   L-68-8526

Figure 12.- Continued.
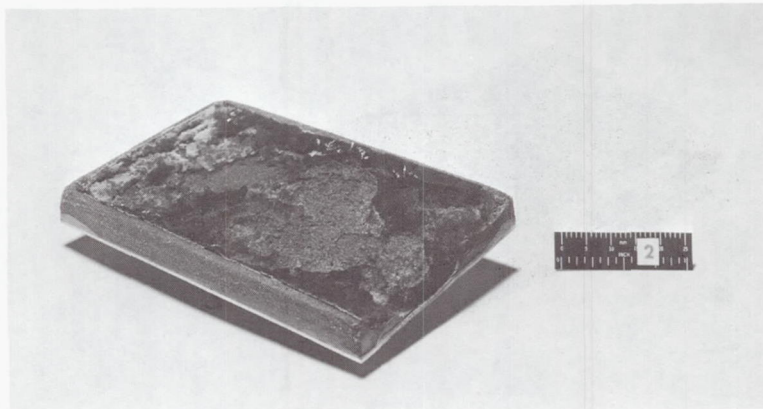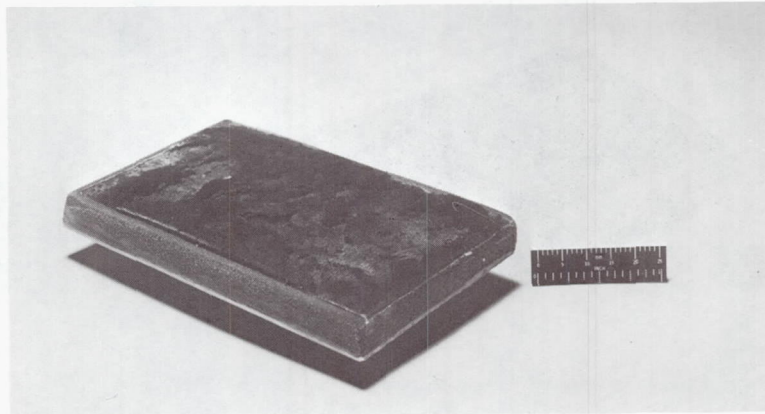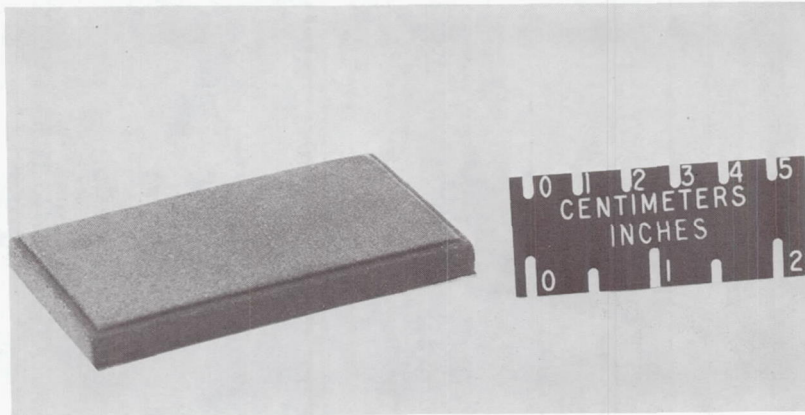
(i) E6A7.   L-68-8527

Figure 12.- Concluded.
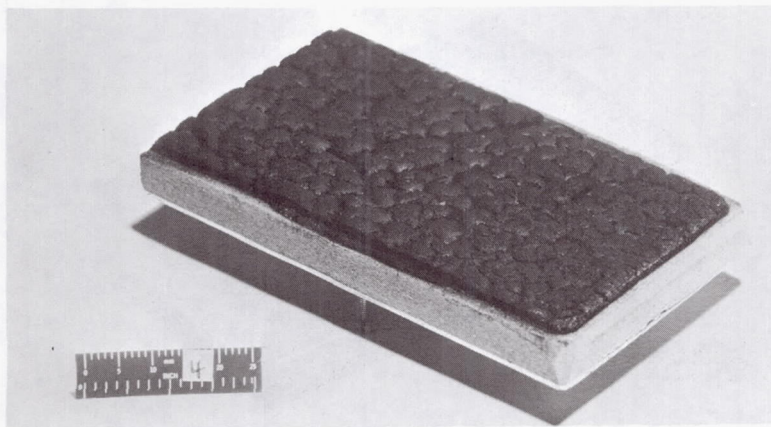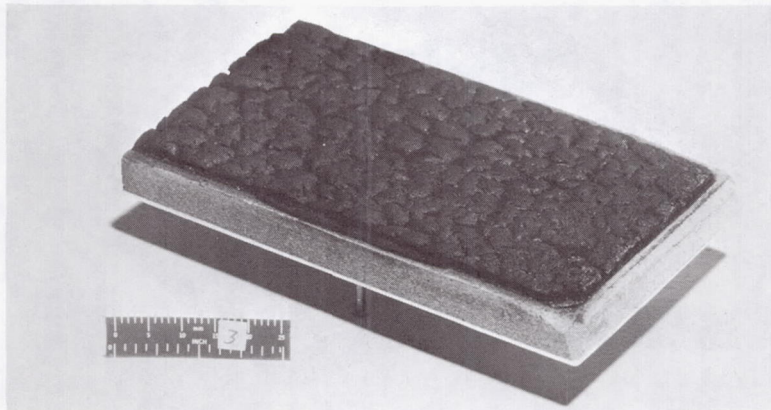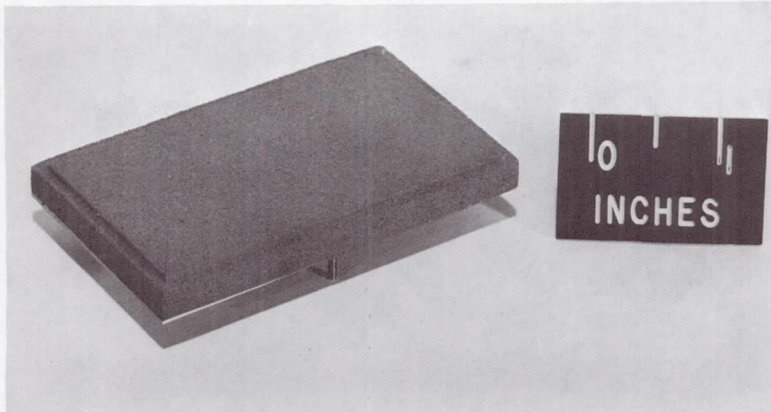
(a) Avco 893-23.   L-68-8528

Figure 13.- Photographs of test specimens before and after exposure to high-heat-transfer (α = 0.49 radian) test condition in arc tunnel.
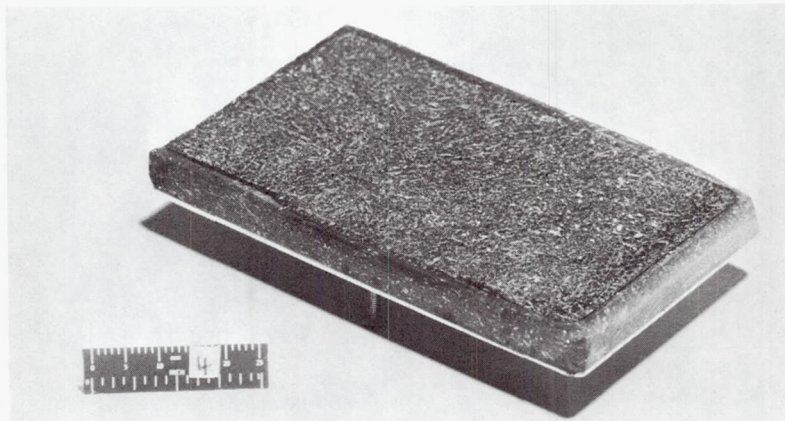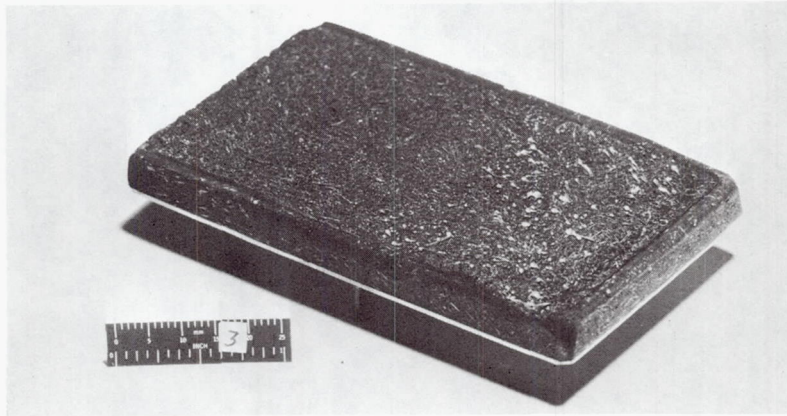
(b) Avcoat 5026-99A.   L-68-8529

Figure 13.- Continued.
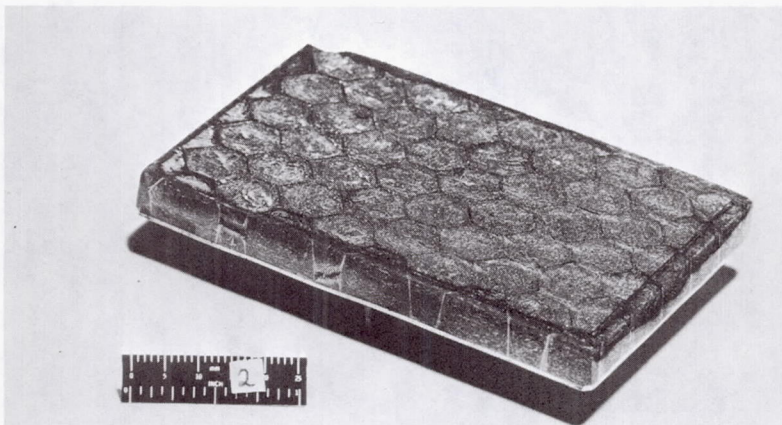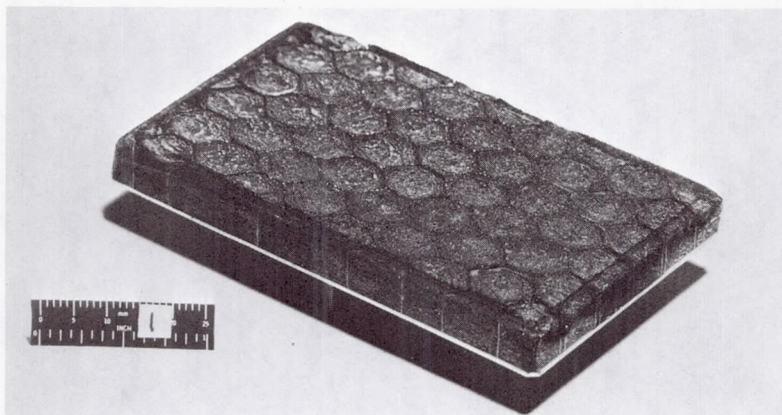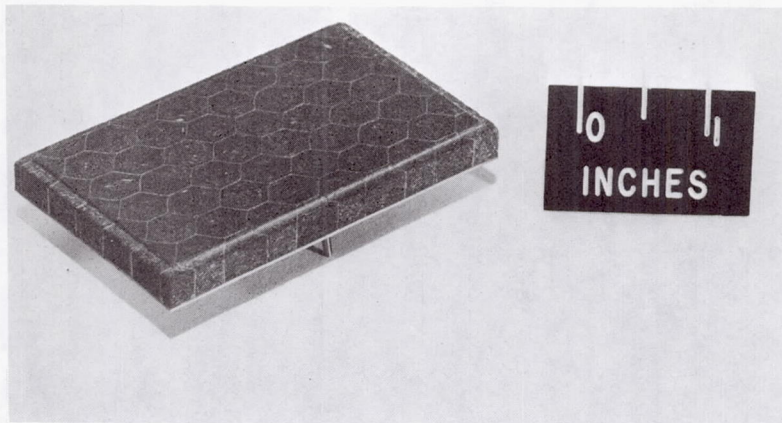
(c) Avcoat 5026-39 HCG.

Figure 13.- Continued.
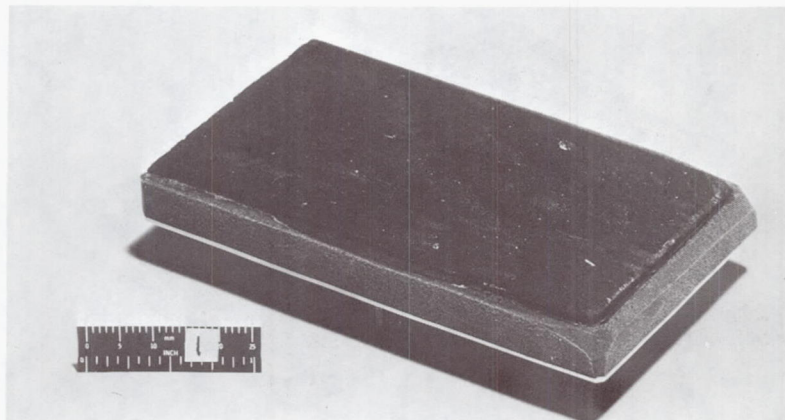
L-68-8530

(d) Avco Mod 7.   L-68-8531
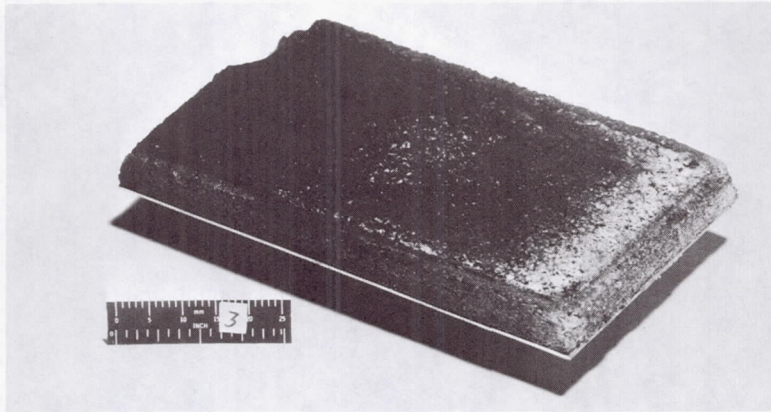
Figure 13.- Continued.
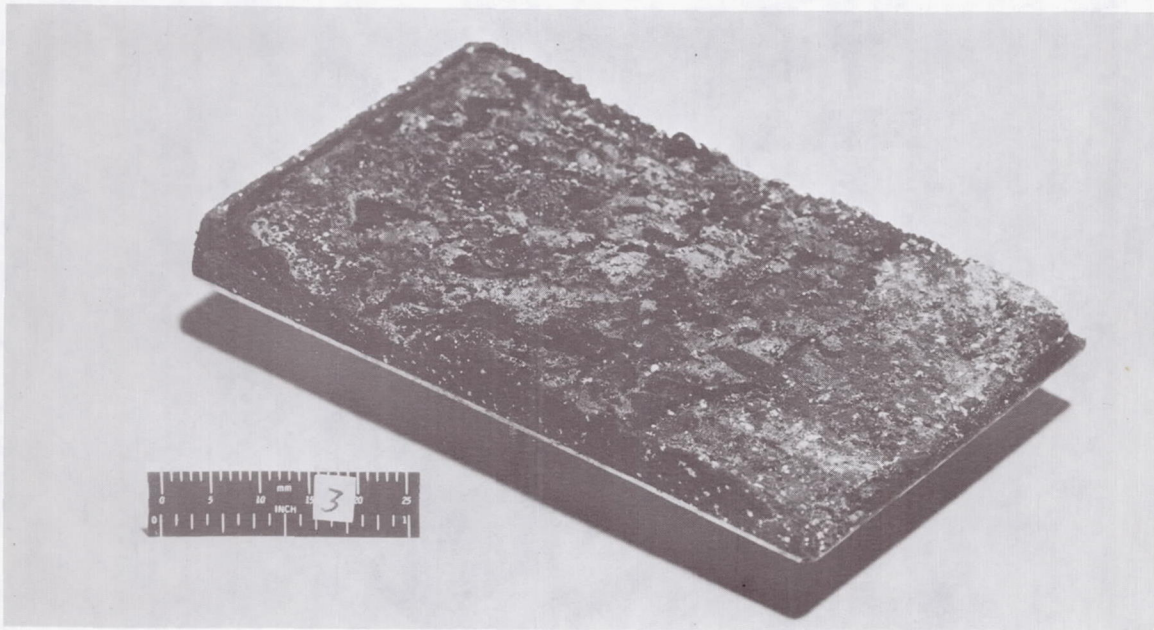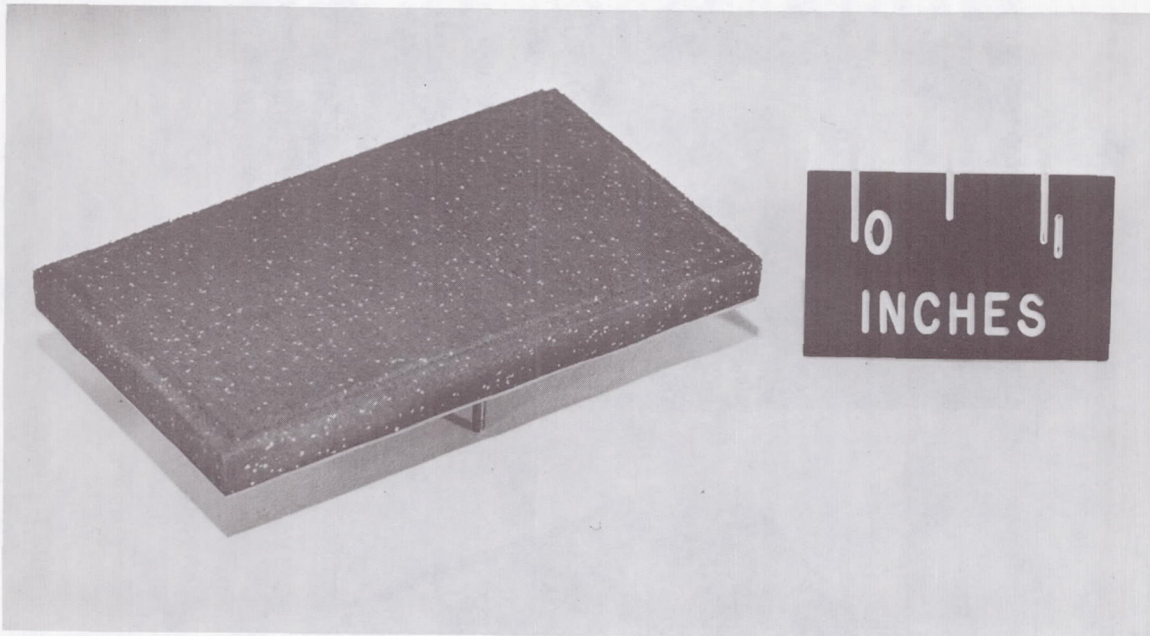
(e) Boeing poly carborazole.   L-68-8532
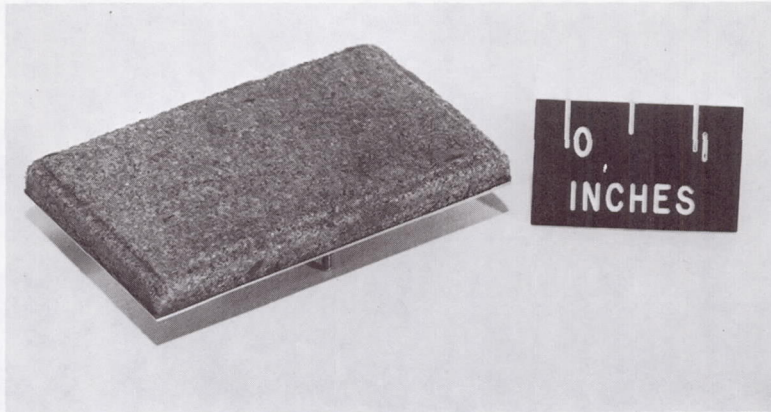
Figure 13.- Continued.
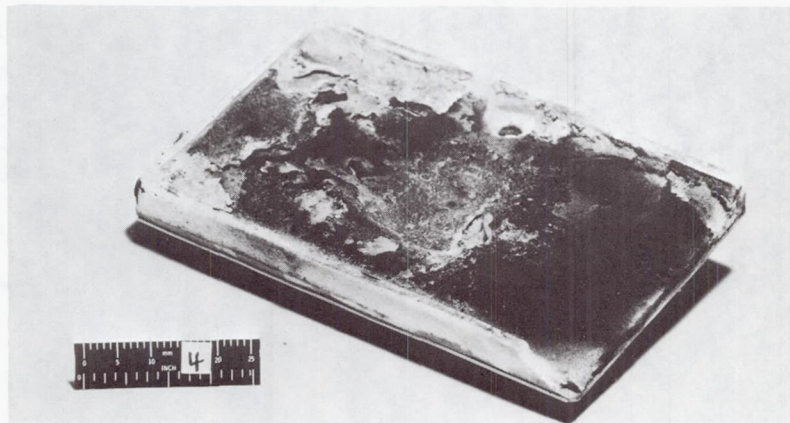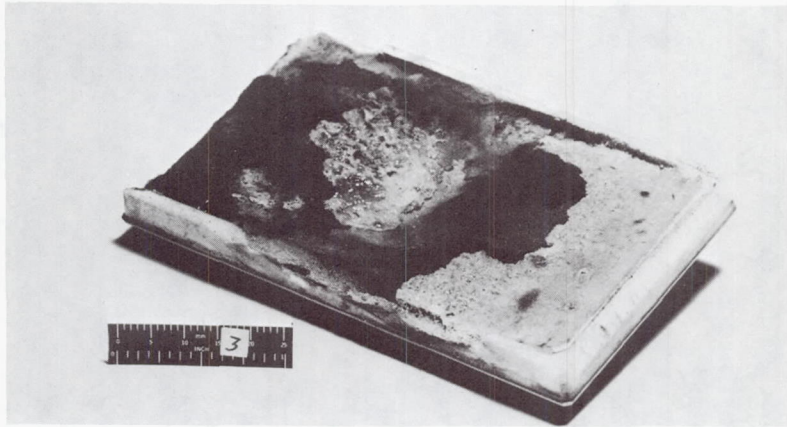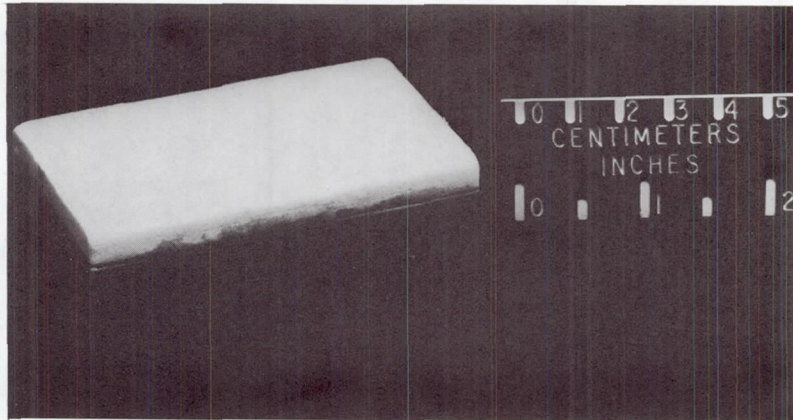
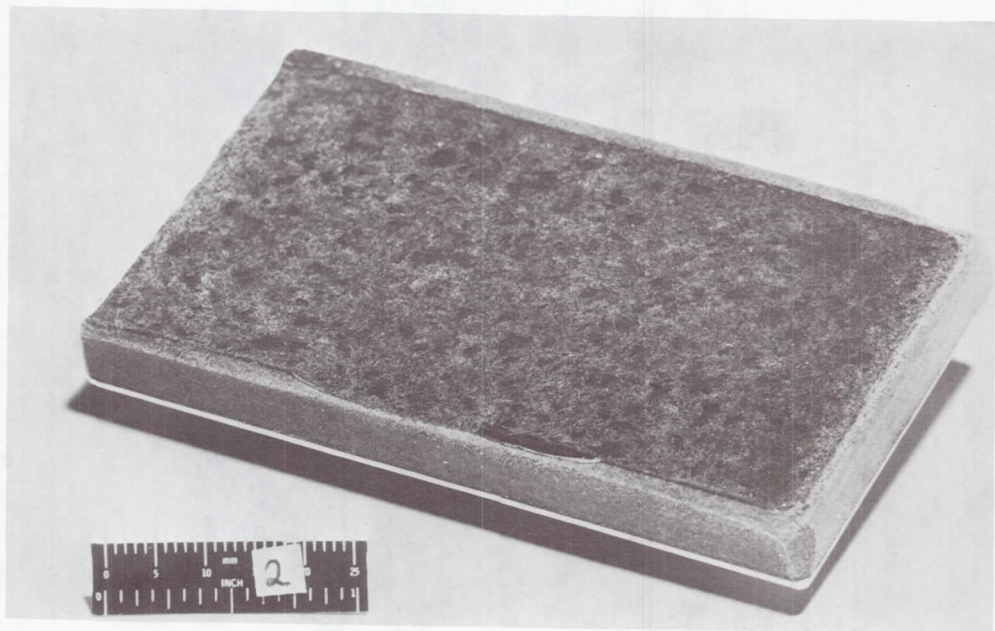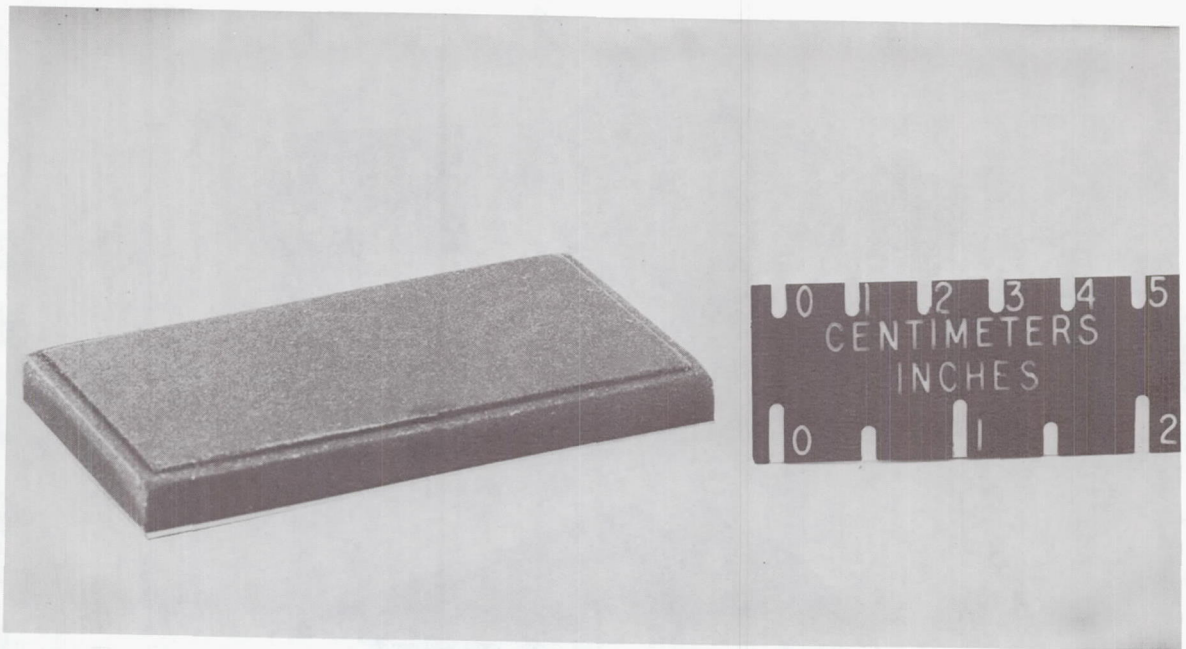(f) Martin SLA-220.   L-68-8533

Figure 13.- Continued.

(g) Martin SLA-561. 　　　　　L-68-8534

Figure 13.- Continued.

(h) E4A1.

L-68-8535

Figure 13.- Concluded.